

---

# OPTIMAL STOPPING FOR SEQUENTIAL BAYESIAN EXPERIMENTAL DESIGN

---

A PREPRINT

 **Chen Cheng**

Department of Mechanical Engineering  
University of Michigan  
Ann Arbor, MI 48109  
chech@umich.edu

 **Xun Huan**

Department of Mechanical Engineering  
University of Michigan  
Ann Arbor, MI 48109  
xhuan@umich.edu

## ABSTRACT

Sequential Bayesian experimental design typically assumes that the number of experiments is fixed before data collection begins. In practical campaigns, however, experimentation may need to terminate early because additional measurements can provide diminishing information relative to their cost, raising the central decision question: *when should one stop?* Common threshold-based stopping rules are easy to implement but myopic, because they compare the current state with a fixed criterion without accounting for the expected value of future experiments. This work develops a Bayesian optimal stopping framework for sequential experimental design by formulating stopping and design as coupled decisions in a Markov decision process. We prove that, for any design policy, the optimal stopping rule terminates exactly when the immediate terminal reward exceeds the expected continuation value. We then derive a policy gradient method for learning value-based stopping and design policies. Naïve joint training can create a circular dependency that traps learning in early-stopping local optima. We address this difficulty with a curriculum learning strategy that gradually transitions from forced continuation to adaptive stopping during training. Numerical studies on a linear-Gaussian benchmark, a one-dimensional nonlinear test problem, and a contaminant source detection problem show that the proposed approach learns stable design–stopping policies and improves resource-aware performance, with the largest gains in settings with strong sequential dependence.

**Keywords** Bayesian experimental design · optimal stopping · Markov decision process · policy gradient · curriculum learning · sequential design

## 1 Introduction

Sequential experimentation plays a central role in science and engineering, from clinical trials (Murphy, 2003) and materials discovery (Lookman, Balachandran, Xue and Yuan, 2019) to environmental monitoring (Krause, Singh and Guestrin, 2008). In these settings, practitioners adaptively choose each new experiment using the outcomes of previous experiments. A fundamental but often overlooked question is therefore inseparable from design itself: *when should experimentation stop?*

Bayesian experimental design (Chaloner and Verdinelli, 1995; Ryan, Drovandi, McGree and Pettitt, 2016; Alexanderian, 2021; Rainforth, Foster, Ivanova and Smith, 2024; Huan, Jagalur and Marzouk, 2024) provides a principled framework for selecting experiments by maximizing expected information gain (Lindley, 1956). Modern sequential extensions (Foster, Ivanova, Malik and Rainforth, 2021; Ivanova, Foster, Kleingessel, Gutmann and Rainforth, 2021; Blau, Bonilla, Chades and Dezfouli, 2022; Shen and Huan, 2023; Shen, Dong and Huan, 2025) adapt each experiment to previously collected data, but they usually assume a fixed experimental horizon: the total number of experiments is specified in advance and no explicit stopping policy is optimized. This assumption is restrictive in practice, where campaigns often face uncertain budgets, limited resources, or diminishing returns that make early termination desirable. Existing early-termination strategies are commonly based on thresholds that stop once a predefined statistic, such as

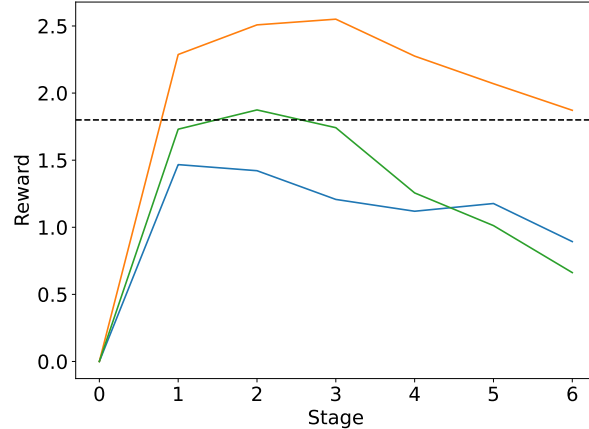


Figure 1: Illustrative accumulated reward trajectories over six experiments, generated from the linear-Gaussian benchmark, showing the limitations of threshold-based stopping. Here, a fixed threshold of 1.8 (dashed line) yields very different outcomes across trajectories: the orange path is stopped prematurely after one experiment, missing the higher rewards achievable at stages 2–3; the blue path never crosses the threshold, leading to unnecessary continuation past its peak; the green path happens to cross the threshold near its maximum, but only by chance. Threshold rules are thus highly outcome-dependent, either stopping too early or too late, and fail to account for the expected value of future experiments.

posterior variance or remaining budget, crosses a cutoff. Related threshold rules also appear in active learning (Zhu, Wang, Hovy and Ma, 2010; Pullar-Strecker, Dost, Frank and Wicker, 2024), multi-armed bandits (Audibert and Bubeck, 2010), and online A/B testing (Daskalakis and Kawase, 2017). Although convenient, these rules are inherently myopic: they depend only on the current state and ignore the expected long-term trade-off between the value of additional information and the cost of further experiments. Consequently, a threshold may terminate too early, missing valuable information, or too late, wasting resources (see Figure 1).

A more principled approach is to make stopping part of the sequential decision problem. This viewpoint leads naturally to a *Bayesian optimal stopping formulation* in which the immediate reward of terminating is compared with the expected value of continuing. Optimal stopping theory is well developed in stochastic processes and dynamic programming (Peskir and Shiryaev, 2006; Shiryaev, 2008; Haggstrom, 1966; Bertsekas, 2012; Puterman, 2014). Existing reinforcement learning formulations of stopping typically use a binary action space {continue, stop}, learning a stopping policy without jointly optimizing the experimental design or control action selected upon continuation (Fathan and Delage, 2021; Li and Lee, 2023). Some Bayesian designs include *ad hoc* termination mechanisms; for example, Berry, Müller, Grieve, Smith, Parke, Blazek, Mitchard and Krams (2002) introduced a “terminator” action in adaptive drug trials using low-dimensional Gaussian approximations and backward induction over small discrete state and action spaces. That approach is valuable but specialized and not information-theoretic. Related ideas also appear in Bayesian optimization (BO), where the Knowledge Gradient (KG) (Frazier, Powell and Dayanik, 2008; Ryzhov, Powell and Frazier, 2012) continues sampling only when the expected one-step improvement exceeds evaluation cost (Garnett, 2023; Xie, Cai, Terenin, Frazier and Scully, 2025). While effective for BO objectives, KG remains a one-step criterion tied to optimization rather than a general information-theoretic formulation for sequential Bayesian experimental design with optimal stopping.

Despite progress in sequential design and optimal stopping as separate topics, a general framework is still missing for jointly optimizing design and stopping in information-theoretic sequential Bayesian experimental design. Simply adding a termination action to an existing sequential design method is not enough, because stopping changes the decision problem by introducing an endogenous horizon, terminal rewards, and a state-dependent stopping boundary. These structural changes create both theoretical and computational challenges. Amortized methods such as Deep Adaptive Design (DAD) (Foster et al., 2021) rely on pathwise gradient estimators for fixed-horizon trajectories with smooth dependence on policy parameters, making discrete termination decisions difficult to incorporate. Conversely, generic reinforcement learning approaches (Blau et al., 2022) can represent stopping in discrete settings, but in continuous design spaces they typically rely on score-function estimators and model stopping as a stochastic action rather than a deterministic value-based decision. Appendix A.6 provides an empirical illustration of this limitation using a generic hybrid-action reinforcement learning baseline. More broadly, naïve joint optimization creates a circular dependency:

the design policy determines future information, the continuation value determines the stopping boundary, and the stopping boundary determines which trajectories are observed during training. This feedback can cause premature termination and poor sample efficiency.

In this work, we address these challenges by developing a rigorous framework for optimal stopping in sequential Bayesian experimental design. Our contributions are:

- We cast sequential design with stopping as a Markov decision process (MDP), jointly optimizing design and stopping policies.
- We prove that the optimal stopping rule is to terminate exactly when the terminal reward exceeds the expected continuation value.
- We introduce a policy gradient algorithm with value-function approximation for learning continuous design policies with value-based stopping.
- We identify a circular dependency that can trap training in early-stopping local optima, and mitigate it using curriculum learning that gradually transitions from forced continuation to adaptive stopping.
- Through a linear-Gaussian benchmark, a one-dimensional nonlinear test problem, and a contaminant source detection problem, we demonstrate stable, resource-aware design–stopping policies, with the largest curriculum gains in settings with strong sequential dependence.

Together, these contributions connect optimal stopping with Bayesian experimental design and provide a foundation for autonomous, resource-aware experimentation.

This paper is structured as follows. Section 2 formulates sequential Bayesian experimental design with stopping as a Markov decision process. Section 3 derives the optimal stopping rule, develops the policy gradient algorithm, and introduces curriculum learning for stabilizing training under circular design–stopping dependencies. Section 4 validates the approach on a linear-Gaussian benchmark, a one-dimensional nonlinear test problem, and a contaminant source detection problem. Section 5 concludes.

## 2 Problem Formulation

### 2.1 Preliminaries

We consider a finite sequence of  $N$  experiments indexed by  $k = 0, 1, \dots, N-1$ . Let  $\theta \in \mathbb{R}^{N_\theta}$  denote model parameters,  $\xi_k \in \Xi_k \subseteq \mathbb{R}^{N_\xi}$  the design for experiment  $k$ , and  $y_k \in \mathbb{R}^{N_y}$  the corresponding observation. The information history at stage  $k$  is  $I_k = \{\xi_0, y_0, \dots, \xi_{k-1}, y_{k-1}\}$  with  $I_0 = \emptyset$ . The stage- $k$  belief (i.e., the prior for experiment  $k$ ) is  $p(\theta | I_k)$ . Observations are assumed to follow

$$y_k = G_k(\theta, \xi_k; I_k) + \epsilon_k, \quad (1)$$

where  $G_k$  is the forward map (which may depend on  $I_k$ ), and  $\epsilon_k$  is an additive observation noise with known density  $p_\epsilon$ . We assume  $\epsilon_k$  is conditionally independent across stages given  $(\theta, \xi_k, I_k)$ . Upon observing  $y_k$ , the belief is updated via Bayes' rule:

$$p(\theta | y_k, \xi_k, I_k) = \frac{p(y_k | \theta, \xi_k, I_k) p(\theta | I_k)}{p(y_k | \xi_k, I_k)}, \quad (2)$$

where  $p(y_k | \theta, \xi_k, I_k)$  is the likelihood induced by  $(G_k, p_\epsilon)$ , and  $p(y_k | \xi_k, I_k) = \int p(y_k | \theta, \xi_k, I_k) p(\theta | I_k) d\theta$  is the marginal likelihood. The posterior  $p(\theta | y_k, \xi_k, I_k)$  then becomes the prior for the next stage, i.e.,  $p(\theta | I_{k+1})$ . This recursive update defines the belief-state dynamics that will underlie our MDP formulation in Section 2.2.

### 2.2 Markov Decision Process for Optimal Stopping

We formulate optimal stopping for sequential Bayesian experimental design as an MDP (see Figure 2). This extends existing MDP-based sequential design frameworks (e.g., Shen and Huan, 2023) by introducing an explicit stopping action that enables early termination of the experimental sequence.

**States.** At stage  $k$ , the state  $s_k \in \mathcal{S}$  is represented as  $s_k = \{s_k^b, s_k^p\}$ . The belief state  $s_k^b$  summarizes the uncertainty about  $\theta$  and is fully determined by  $I_k$ ; for this paper, we can equivalently view  $s_k = I_k$ , yielding a Markov state representation. The physical state  $s_k^p$  captures any additional deterministic variables relevant to design (e.g., sensor positions). An additional special terminal state  $T$  indicates that the experimental sequence has stopped and no future experiments will be conducted.

**Actions and policies.** At each stage, the agent either (i) terminates the design process, or (ii) chooses a design  $\xi_k \in \Xi_k$  to perform an experiment. The stopping policy is a collection of binary decision rules,  $\psi = \{\varphi_k : \mathcal{S} \rightarrow \{0, 1\}, k =$

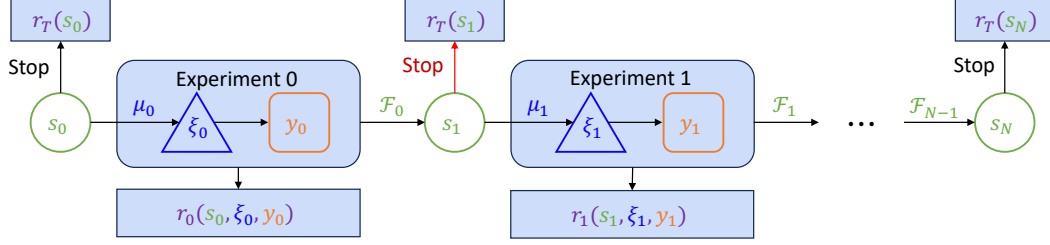


Figure 2: Flowchart of the MDP for sequential Bayesian experimental design with optimal stopping. At each stage, the agent chooses to continue or stop. If continuing, the design policy selects an experiment, yielding an observation and reward, and the state is updated via Bayes' rule. If stopping, a terminal reward is collected. The process repeats until termination or all experiments are exhausted.

$0, \dots, N-1$ }, where  $\varphi_k(s_k) = 1$  indicates stopping at stage  $k$ . The design policy is a collection of mappings  $\pi = \{\mu_k : \mathcal{S} \rightarrow \Xi_k, k = 0, \dots, N-1\}$ , which determine designs via  $\xi_k = \mu_k(s_k)$ .

**State transitions.** When an experiment is performed, the state evolves according to  $s_{k+1} = \mathcal{F}_k(s_k, \xi_k, y_k)$ , which encodes the Bayesian update in (2) given observation  $y_k$ . If the termination action is selected, or if all  $N$  experiments have been exhausted, the state transitions to the terminal state  $T$ , where it remains thereafter. Formally,

$$s_{k+1} = \begin{cases} \mathcal{F}_k(s_k, \xi_k, y_k), & s_k \neq T \text{ and } \varphi_k(s_k) = 0, \\ T, & \text{otherwise.} \end{cases} \quad (3)$$

This transition structure induces an endogenous (state-dependent) horizon determined by the stopping policy.

**Rewards.** The reward encodes information gain and experimental cost. Let  $r_k(s_k, \xi_k, y_k)$  denote the immediate reward at stage  $k$ , and  $r_T(s_k)$  the terminal reward collected when the experimental sequence ends. Experiment  $k$  incurs a (negative) cost  $c_k(\xi_k)$ . Information gain is measured using the Kullback–Leibler (KL) divergence between distributions. We consider two equivalent reward formulations:

- *Terminal formulation* (all rewards are accumulated at termination):

$$r_k(s_k, \xi_k, y_k) = 0, \quad (4)$$

$$r_T(s_k) = \begin{cases} D_{\text{KL}}(p_{\theta|I_k} || p_{\theta|I_0}) + \sum_{i=0}^{k-1} c_i(\xi_i), & s_k \neq T \text{ and } \varphi_k(s_k) = 1, \\ 0, & \text{otherwise.} \end{cases} \quad (5)$$

- *Incremental formulation* (rewards distributed across stages):

$$r_k(s_k, \xi_k, y_k) = \begin{cases} D_{\text{KL}}(p_{\theta|I_{k+1}} || p_{\theta|I_k}) + c_k(\xi_k), & s_k \neq T \text{ and } \varphi_k(s_k) = 0, \\ 0, & \text{otherwise,} \end{cases} \quad (6)$$

$$r_T(s_k) = 0. \quad (7)$$

**Problem statement.** The goal is to find optimal design and stopping policies:

$$\pi^*, \psi^* \in \arg \max_{\pi, \psi} U(\pi, \psi) \quad (8)$$

subject to

$$\varphi_k(s_k) \in \{0, 1\}, \quad \xi_k = \mu_k(s_k) \in \Xi_k,$$

$$s_{k+1} = \begin{cases} \mathcal{F}_k(s_k, \xi_k, y_k), & s_k \neq T \text{ and } \varphi_k(s_k) = 0, \\ T, & \text{otherwise.} \end{cases}$$

where the objective (expected utility) is the expected total reward:

$$U(\pi, \psi) = \mathbb{E}_{y_{0:N-1} | \pi, \psi, s_0} \left[ \sum_{k=0}^{N-1} (r_k(s_k, \xi_k, y_k) + r_T(s_k)) + r_T(s_N) \right]. \quad (9)$$

Although the terminal and incremental formulations differ in reward structure, they induce equivalent optimal policies when maximizing expected total reward. This MDP formulation unifies design and stopping as joint decision variables, providing a principled framework for resource-efficient experimentation.

### 3 Solution Method

This section develops the computational framework for learning sequential designs with optimal stopping. We first characterize the value-based stopping rule induced by any fixed design policy. We then use this structure to reduce joint design–stopping optimization to a policy gradient update over the continuous design policy, with a critic network estimating the continuation value. Finally, we introduce a curriculum strategy that stabilizes training by delaying the influence of learned stopping decisions until the design and value networks have observed sufficiently informative trajectories.

#### 3.1 Optimal stopping policy

We begin by defining the value function used to compare stopping and continuation. The V-function at stage  $k$  ( $k = 0, \dots, N - 1$ ) under design policy  $\pi$  and stopping policy  $\psi$  is:

$$V_k^{\pi, \psi}(s_k) = \mathbb{E}_{y_k: N-1 | \pi, \psi, s_k} \left[ \sum_{l=k}^{N-1} (r_l(s_l, \mu_l(s_l), y_l) + r_T(s_l)) + r_T(s_N) \right], \quad (10)$$

which represents the expected cumulative reward from state  $s_k$  onward when following  $\pi$  and  $\psi$ . Equivalently, the value function satisfies the recursion  $V_k^{\pi, \psi}(s_k) = \mathbb{E}_{y_k | \pi, \psi, s_k} [r_k(s_k, \mu_k(s_k), y_k) + r_T(s_k) + V_{k+1}^{\pi, \psi}(s_{k+1})]$  with  $V_N^{\pi, \psi}(s_N) = r_T(s_N)$ .

Define  $r_T^S(s_k)$  as the terminal reward obtained by stopping at  $s_k$  (i.e.,  $s_k \neq T$  and  $\varphi_k(s_k) = 1$ ), and  $r_k^C(s_k, \mu_k(s_k), y_k)$  as the immediate reward obtained by continuing (i.e.,  $s_k \neq T$  and  $\varphi_k(s_k) = 0$ ).

**Theorem 3.1** (Optimal Stopping Policy). *For any design policy  $\pi = \{\mu_0, \dots, \mu_{N-1}\}$ , the optimal stopping policy is  $\psi = \{\varphi_0, \dots, \varphi_{N-1}\}$  with*

$$\varphi_k(s_k) = \mathbf{1}_{s_k \in \mathcal{T}_k}, \quad k = 0, \dots, N - 1, \quad (11)$$

where the stopping set  $\mathcal{T}_k \subseteq \mathcal{S}$  is defined as:

$$\mathcal{T}_k = \left\{ s_k \mid r_T^S(s_k) \geq \mathbb{E}_{y_k | s_k, \pi} \left[ r_k^C(s_k, \mu_k(s_k), y_k) + V_{k+1}^{\pi, \psi}(\mathcal{F}_k(s_k, \mu_k(s_k), y_k)) \right] \right\}. \quad (12)$$

We provide a proof in Appendix A.1. The theorem states that the optimal decision at each stage is a value comparison: stop if the terminal reward is no smaller than the expected value of conducting one more experiment and then acting optimally. This rule balances the value of ending experimentation immediately against the potential information gain from future experiments.

To formalize this comparison, we define a specialized action-value function (Q-function) that evaluates the return when the next action is to continue—the *value of continuation*—after which  $\pi$  and  $\psi$  are followed:

$$Q_k^{\pi, \psi}(s_k, \xi_k) = \mathbb{E}_{y_k | s_k, \xi_k} \left[ r_k^C(s_k, \xi_k, y_k) + V_{k+1}^{\pi, \psi}(s_{k+1}) \right], \quad (13)$$

where  $s_{k+1} = \mathcal{F}_k(s_k, \xi_k, y_k)$ . The stopping set can be expressed equivalently and succinctly as:

$$\mathcal{T}_k = \left\{ s_k \mid r_T^S(s_k) \geq Q_k^{\pi, \psi}(s_k, \mu_k(s_k)) \right\}. \quad (14)$$

Thus the Q-function provides a direct criterion for deciding whether the terminal reward is preferable to the value of continuation.

**Theorem 3.2** (Terminal-Incremental Equivalence With Stopping). *Let  $U_T(\pi, \psi)$  denote the expected utility under the terminal formulation in (4) and (5), and  $U_I(\pi, \psi)$  the expected utility under the incremental formulation in (6) and (7). Then for any policies  $(\pi, \psi)$ ,  $U_T(\pi, \psi) = U_I(\pi, \psi)$ .*

We provide a proof in Appendix A.2. While terminal–incremental equivalence is known for fixed-horizon sequential design (Foster et al., 2021; Shen and Huan, 2023), extending this result to settings with policy-dependent stopping requires explicitly proving consistency of optimal stopping across both formulations. This extension is important computationally because it ensures that both reward formulations yield equivalent optimal policies while allowing implementation choices that trade off reward sparsity against per-stage posterior computations. We return to this tradeoff in Section 3.2.

### 3.2 Policy gradient for optimal stopping

Theorem 3.1 shows that the optimal stopping policy is implicitly determined by the design policy  $\pi$ . This suggests that the joint optimization problem can be reformulated as a single optimization over the design policy alone. We therefore parameterize the design policy, derive the gradient of the expected utility with respect to its parameters, and employ gradient-based optimization. This leads to a policy gradient (PG) method, which directly optimizes the design policy by differentiating the expected utility with respect to its parameters (Silver, Lever, Heess, Degris, Wierstra and Riedmiller, 2014; Wang, Cai, Yang and Wang, 2020).

#### 3.2.1 Policy gradient derivation

We parameterize each design function  $\mu_k$  with parameters  $w_k$ , and write  $\mu_{k,w_k}$ . The full design policy  $\pi$  is parameterized by  $w = \{w_k\}_{k=0}^{N-1}$ , denoted  $\pi_w$ . The corresponding stopping policy is implicitly determined by  $w$  as  $\psi_w$ , with

$$\varphi_{k,w}(s_k) = \mathbf{1}_{s_k \in \mathcal{T}_{k,w}}, \quad (15)$$

where the stopping set  $\mathcal{T}_{k,w}$  is defined by:

$$\begin{aligned} \mathcal{T}_{k,w} &= \left\{ s_k \mid r_T^S(s_k) \geq \mathbb{E}_{y_k | \pi_w, s_k} \left[ r_k^C(s_k, \mu_{k,w_k}(s_k), y_k) + V_{k+1}^{\pi_w, \psi_w}(\mathcal{F}_k(s_k, \mu_{k,w_k}(s_k), y_k)) \right] \right\} \\ &= \left\{ s_k \mid r_T^S(s_k) \geq Q_k^{\pi_w, \psi_w}(s_k, \mu_{k,w_k}(s_k)) \right\}. \end{aligned} \quad (16)$$

The expected utility (9) becomes:

$$U(w) = \mathbb{E}_{y_{0:N-1} | \pi_w, \psi_w, s_0} \left[ \sum_{k=0}^{N-1} (r_k(s_k, \mu_{k,w_k}(s_k), y_k) + r_T(s_k)) + r_T(s_N) \right]. \quad (17)$$

**Theorem 3.3** (Policy Gradient). *The gradient of the expected utility with respect to the design policy parameters is:*

$$\nabla_w U(w) = \sum_{k=0}^{N-1} \mathbb{E}_{s_k | \pi_w, \psi_w, s_0} \left[ \mathbf{1}_{k < \tau_w} \nabla_w \mu_{k,w_k}(s_k) \cdot \nabla_{\xi_k} Q_k^{\pi_w, \psi_w}(s_k, \xi_k) \Big|_{\xi_k = \mu_{k,w_k}(s_k)} \right] \quad (18)$$

where  $\tau_w = \inf\{k : \varphi_{k,w}(s_k) = 1\}$  is the stage when the state first enters the stopping set.

We provide a proof in Appendix A.3.

#### 3.2.2 Numerical estimation

The gradient in Theorem 3.3 involves nested expectations over stochastic trajectories and stopping decisions, which are intractable in closed form. We therefore use a Monte Carlo estimator:

$$\nabla_w U(w) \approx \frac{1}{M} \sum_{m=1}^M \sum_{k=0}^{N-1} \mathbf{1}_{k < \tau^{(m)}} \nabla_w \mu_{k,w_k}(s_k^{(m)}) \cdot \nabla_{\xi_k^{(m)}} Q_k^{\pi_w, \psi_w}(s_k^{(m)}, \xi_k^{(m)}) \Big|_{\xi_k^{(m)} = \mu_{k,w_k}(s_k^{(m)})} \quad (19)$$

where superscript indicates the  $m$ th sampled trajectory.

Two computational challenges arise: policy gradients  $\nabla_w \mu_{k,w_k}$  must be evaluated efficiently, and Q-function gradients  $\nabla_{\xi} Q_k^{\pi_w, \psi_w}$  cannot be estimated reliably by nested Monte Carlo because such estimates would have high variance and prohibitive cost. We address both challenges with an actor-critic approximation (Sutton and Barto, 2018). The actor represents the design policy and is updated using the policy gradient estimator in (19), while the critic approximates the continuation value and supplies differentiable, lower-variance gradient information for improving the actor.

#### 3.2.3 Actor-Critic Implementation

**Policy network.** The design policy is parameterized by a single deep neural network  $\mu_w(k, s_k)$  that takes as input both the current stage index  $k$  and state  $s_k$ . Since the history grows in length across stages, we use a fixed-size, zero-padded representation as in Shen and Huan (2023). The stage index is encoded as a one-hot vector,

$$k \quad \longrightarrow \quad e_{k+1} = [0, \dots, 0, \underbrace{1}_{(k+1)\text{th}}, 0, \dots, 0]^T, \quad (20)$$

and the state  $s_k$  is represented in a nonparametric manner with the experimental history  $I_k$ ,

$$s_k \longrightarrow I_k = \{\xi_0, y_0, \dots, \xi_{k-1}, y_{k-1}\}, \quad (21)$$

which is laid out sequentially and zero-padded (for experiments that have not happened yet) to a fixed dimension  $(N-1)(N_\xi + N_y)$ . The complete input vector at stage  $k$  is

$$\left[ \underbrace{e_{k+1}}_N, \underbrace{\xi_0, \dots, \xi_{k-1}}_{N_\xi}, \underbrace{0, \dots, 0}_{N_\xi(N-1-k)}, \underbrace{y_0, \dots, y_{k-1}}_{N_y}, \underbrace{0, \dots, 0}_{N_y(N-1-k)} \right]^T, \quad (22)$$

giving a total input dimension of  $N + (N-1)(N_\xi + N_y)$ . The output is an  $N_\xi$ -dimensional vector representing the proposed design  $\xi_k$ . Gradients  $\nabla_w \mu_{k,w_k}(s_k^{(m)}) = \nabla_w \mu_w(k, s_k^{(m)})$  are computed via standard backpropagation.

**Q-network.** To approximate the continuation value defined in (13), we train a neural network  $Q_\eta^{\pi_w, \psi_w}(k, s_k, \xi_k)$  with parameters  $\eta$ . This avoids costly inner Monte Carlo sampling for directly estimating  $Q$  and provides differentiable Q-function estimates. The Q-network shares the same input structure as the policy network but additionally takes the candidate design  $\xi_k$ , giving total input dimension  $N + (N-1)(N_\xi + N_y) + N_\xi$ ; the output is a scalar representing the expected continuation value. The Q-network is trained by minimizing:

$$\mathcal{L}(\eta) = \frac{1}{M} \sum_{m=1}^M \sum_{k=0}^{N-1} \left[ Q_\eta^{\pi_w, \psi_w}(k, s_k^{(m)}, \xi_k^{(m)}) - r_k(s_k^{(m)}, \xi_k^{(m)}, y_k^{(m)}) - Q_{k+1}^{\pi_w, \psi_w}(s_{k+1}^{(m)}, \xi_{k+1}^{(m)}) \right]^2 \mathbf{1}_{k < \tau^{(m)}}, \quad (23)$$

with  $\xi_k^{(m)} = \mu_w(k, s_k^{(m)})$  and  $Q_N^{\pi_w, \psi_w}(s_N^{(m)}, \cdot) = r_T(s_N^{(m)})$ . This loss enforces the Bellman equation and ensures accurate return predictions.

**Training.** We follow a standard actor-critic loop in Algorithm 1. During training, each episode is generated by first sampling a parameter  $\theta^{(m)} \sim p(\theta)$ . The design policy  $\mu_k(s_k)$  itself is deterministic; however, to encourage exploration during trajectory generation, we inject a small perturbation into the design when generating the Monte Carlo samples used for gradient estimation:

$$\xi_k = \mu_k(s_k) + \epsilon_{\text{explore}}, \quad \epsilon_{\text{explore}} \sim \mathcal{N}(0, \mathbb{I}_{N_\xi} \sigma_{\text{explore}}^2). \quad (24)$$

The value of  $\sigma_{\text{explore}}$  reflects the degree of exploration and should be selected based on the problem context. A common practice is to set a large  $\sigma_{\text{explore}}$  early in training and reduce it gradually. Stopping is triggered deterministically when  $r_T^S(s_k)$  exceeds the continuation value  $Q_k^{\pi_w, \psi_w}(s_k, \mu_k(s_k))$  in (13). Policy parameters  $w$  are updated via gradient ascent using the Monte Carlo gradient estimator in (19), while Q-network parameters  $\eta$  are updated via stochastic gradient descent on the loss in (23).

**Information gain computation.** The terminal reward calculation requires computing KL divergences between posterior distributions. For problems without analytical posteriors, we approximate these quantities by discretizing the parameter space  $\theta$  on a regular grid and estimating posterior densities pointwise. Figure 3 demonstrates the accuracy of this grid-based approximation in the linear-Gaussian case, where we compare the approximated posterior against the analytical solution. The close agreement validates that grid-based computation provides sufficient accuracy for reward evaluation in our experiments.

In implementation, the choice between terminal and incremental formulations involves a computational tradeoff. In the terminal-reward formulation, all intermediate rewards are zero, providing sparse supervision to the critic. This can slow convergence early in training, as the Bellman loss (23) receives gradient signal only from episodes that reach the stopping decision. Conversely, the incremental formulation provides denser reward signals at each stage, which can accelerate learning. However, this comes at the cost of computing information gains in  $r_k(\cdot)$  at every stage, which is computationally expensive for high-dimensional posteriors and introduces approximation errors in intermediate posterior updates. In practice, the choice depends on the available computational budget and desired learning dynamics. In our experiments, we adopt the terminal formulation for its simplicity and transparent interpretation of the cumulative reward.

Algorithm 1 summarizes the resulting training procedure.

### 3.3 Training instabilities and curriculum learning

Although the PG method provides a principled framework, direct training can be unstable because stopping and continuation values are mutually dependent. The optimal stopping set  $\mathcal{T}_k$  in (14) depends on the continuation value

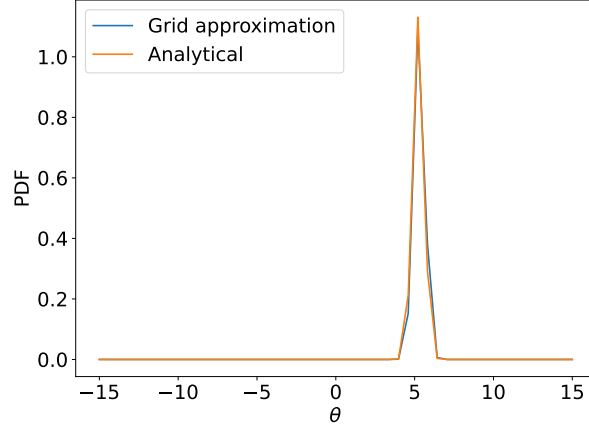


Figure 3: Comparison of grid-based posterior approximation against the analytical Gaussian posterior in the linear-Gaussian benchmark.

---

**Algorithm 1** Actor-critic PG for optimal stopping.

---

- 1: Set initial state  $s_0$ , policy updates  $L$ , sample size  $M$ , policy and Q-network architectures, learning rate  $\alpha$  for policy update, exploration scale  $\sigma_{\text{explore}}$ ;
  - 2: Initialize policy and Q-network parameters  $w$  and  $\eta$ ;
  - 3: **for**  $\ell = 1, \dots, L$  **do**
  - 4:   Simulate  $M$  episodes with path  $m = 1, \dots, M$  following steps 5–10 below;
  - 5:   Initialize  $s_0^{(m)} = s_0$  and sample  $\theta^{(m)} \sim s_{0,b}$ ;
  - 6:   **for**  $k = 0, \dots, N - 1$  **do**
  - 7:     Sample design  $\xi_k^{(m)} = \mu_w(k, s_k^{(m)}) + \epsilon_{\text{explore}}$  and  $y_k^{(m)} \sim p(\cdot \mid \theta^{(m)}, \xi_k^{(m)}, I_k^{(m)})$ ;
  - 8:     Update state  $s_{k+1}^{(m)}$ , and compare  $r_T^S(s_{k+1}^{(m)})$  with the learned continuation value  $Q_{\eta}^{\pi, \psi}(k + 1, s_{k+1}^{(m)}, \mu_w(k + 1, s_{k+1}^{(m)}))$  for stopping decision;
  - 9:     If  $s_{k+1}^{(m)} \in \mathcal{T}_{k+1, w}^{(m)}$  or  $k + 1 = N$ , set  $\tau^{(m)} = k + 1$  and exit the loop;
  - 10:   **end for**
  - 11:   Store the full information history from all episodes  $\{I_{\tau^{(m)}}^{(m)}\}_{m=1}^M$ ;
  - 12:   Compute and store immediate and terminal rewards for all episodes  $\{r_k^{(m)}, r_T^{(m)}\}_{m=1}^M$ ;
  - 13:   Update  $\eta$  by minimizing the loss in (23);
  - 14:   Update  $w$  by gradient ascent:  $w = w + \alpha \nabla_w U(w)$ , where  $\nabla_w U(w)$  is estimated via (19);
  - 15: **end for**
  - 16: Return optimized design policy  $\pi_w$  and stopping policy  $\psi_{w, \eta}$ .
- 

$Q_k^{\pi, \psi}(s_k, \mu_k(s_k))$ , which is itself defined under the same design and stopping policies  $(\pi, \psi)$ . Consequently, the stopping policy requires a Q-function computed under that very policy, inducing a fixed-point relationship  $\psi^* = f(\pi, \psi^*)$ .

In practice, this circularity manifests during joint training of the policy network (parameters  $w$ ) and the Q-network (parameters  $\eta$ ). Early in training, the design policy is inevitably inaccurate, producing weak experiments with limited information gain. The Q-network then learns pessimistic continuation values, which induce premature stopping and truncate trajectories before informative designs can be discovered. When the reward landscape contains multiple attraction basins associated with different stopping stages, this feedback can bias learning toward an early-stopping basin before the policy has explored trajectories that lead to higher long-horizon rewards. As a result, the circular dependency can trap training in a suboptimal early-stage policy and cause it to miss a better, or even globally optimal, design–stopping strategy. This issue is particularly pronounced in problems with strong sequential dependencies, where early stopping disrupts the learning of long-horizon experimental strategies.

To overcome this challenge, we adopt a simple form of *curriculum learning*, originally introduced by Bengio, Louradour, Collobert and Weston (2009), in which an algorithm is gradually exposed to increasingly difficult aspects of the task. We

implement this through a stopping probability schedule  $p_{\text{stop}}(\ell)$ , where  $\ell$  indexes training iterations. When the stopping condition  $s_k \in \mathcal{T}_k$  is satisfied, the algorithm follows the optimal stopping rule with probability  $p_{\text{stop}}(\ell)$ , and overrides it (forcing continuation) with probability  $(1 - p_{\text{stop}}(\ell))$  *during training only*. This strategy deliberately relaxes stopping early in training, producing longer trajectories that allow both the policy and Q-networks to improve before stopping decisions dominate the data distribution. As training progresses,  $p_{\text{stop}}(\ell)$  is gradually increased, ensuring that the learned policies converge to the optimal stopping fixed point. In this way, curriculum learning breaks the self-reinforcing cycle of premature stopping and stabilizes training, particularly in settings with strong sequential dependencies.

In Section 4, we empirically examine when this curriculum strategy is beneficial. The clearest gains arise in a movement-constrained source detection problem, where premature stopping prevents the policy from learning informative later-stage designs.

### 3.4 Computational Considerations

The policy gradient method relies on Monte Carlo trajectory simulation during training to estimate gradients. The primary computational costs arise from evaluating information-theoretic rewards (KL divergences between posterior distributions) and forward model evaluations. For low-dimensional parameter spaces ( $N_\theta \leq 4$ ), we employ grid-based discretization to compute posteriors and KL divergences, which is both efficient and transparent. For higher-dimensional problems, practitioners can instead leverage well-established approximation techniques, such as variational inference (Foster, Jankowiak, Bingham, Horsfall, Teh, Rainforth and Goodman, 2019), MCMC-based density estimation, or amortized posterior inference via diffusion models (Baldassari, Siahkoohi, Garnier, Solna and de Hoop, 2023), depending on problem structure and available computational resources.

Once trained, the learned policies enable computationally efficient decision-making at deployment. Determining the next design and stopping decision requires only a single forward pass through the policy and Q-networks, together with one posterior update and forward model evaluation. This eliminates the need for expensive online planning or repeated forward simulations, making the approach well suited for real-time sequential experimentation, even in resource-constrained settings.

## 4 Numerical Experiments

We evaluate the proposed framework on three numerical examples designed to test increasingly difficult aspects of the method. The linear-Gaussian benchmark validates the policy gradient algorithm against analytical solutions. The one-dimensional nonlinear problem tests non-conjugate Bayesian updating while retaining transparent posterior computation. The contaminant source detection problem introduces constrained sensor movement and stronger sequential dependence, making it a stress test for the curriculum strategy. Training hyperparameters are reported in Appendix A.5; they largely follow Shen and Huan (2023). Further hyperparameter tuning may improve performance but is not pursued here.

In our implementation, we adopt an adaptive sigmoid-based schedule to control the gradual increase of  $p_{\text{stop}}(\ell)$ . Specifically, we apply a shifted and scaled sigmoid function of the form:

$$p_{\text{stop}}(\ell) = \frac{1}{1 + \exp(-a(\ell - \ell_0))} \quad (25)$$

where  $a$  controls the transition steepness and  $\ell_0$  determines the midpoint. We set parameters such that  $p_{\text{stop}}(\ell)$  starts near zero, increases smoothly through mid-training, and saturates above 0.999 for the final 30 iterations to guarantee convergence to the optimal stopping policy. This sigmoid-based schedule provides a smooth transition that balances exploration during early training with stability near convergence, avoiding the abrupt changes that can destabilize actor-critic learning.

### 4.1 Linear-Gaussian Benchmark

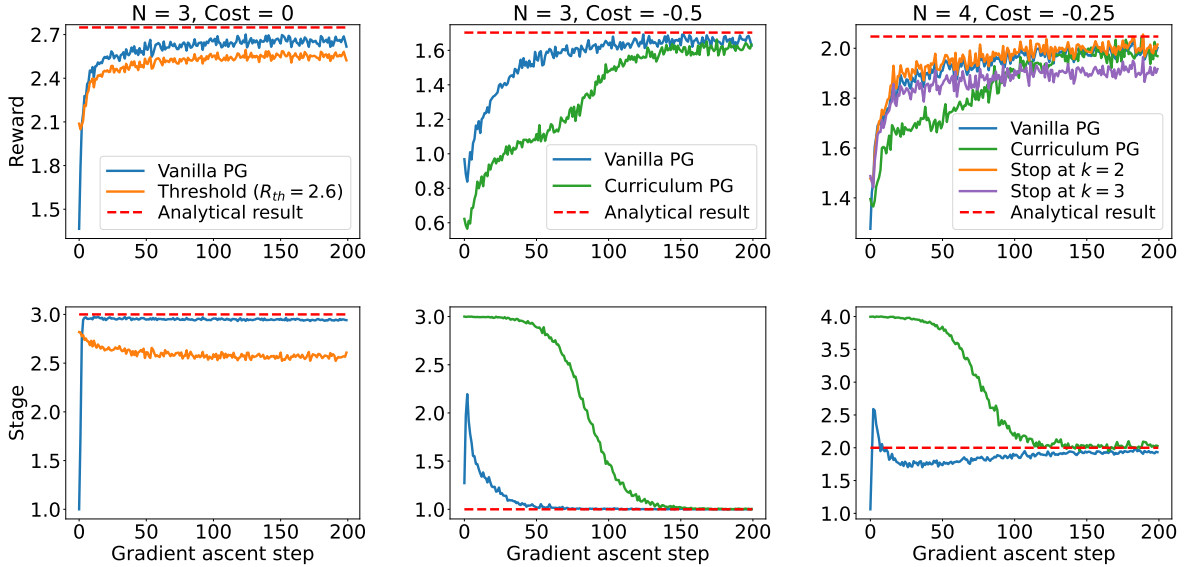
We first validate our PG algorithm on a canonical linear-Gaussian benchmark where analytical solutions are available. The forward model is linear in  $\theta$  with additive Gaussian noise:

$$y_k = G(\theta, \xi_k) + \epsilon_k = \theta \xi_k + \epsilon_k, \quad \epsilon_k \sim \mathcal{N}(0, 1^2), \quad (26)$$

with prior  $\theta \sim \mathcal{N}(0, 3^2)$ . Experiments are constrained to designs  $\xi_k \in [0.1, 3]$ . Conjugacy enables closed-form characterization of optimal stopping and design policies (see Appendix A.4 for detailed derivation). We list the optimal utilities for varying number of experiments in Table 1. The optimal stopping stages are highlighted in red.

Table 1: Analytical optimal utility under varying experimental horizons and costs for the linear-Gaussian benchmark.

$N$	1	2	3	4
$U(\Xi_N)(c_k = 0)$	2.203	2.547	2.749	<b>2.892</b>
$U(\Xi_N)(c_k = -0.5)$	<b>1.703</b>	1.547	1.249	0.892
$U(\Xi_N)(c_k = -0.25)$	1.953	<b>2.047</b>	1.999	1.892

Figure 4: Training convergence of the linear-Gaussian benchmark. Top: average reward; bottom: average stopping stage. Columns correspond to different horizons  $N$  and experimental costs.

For zero cost ( $c_k = 0$ ), the analytical solution shows that stopping is always optimal at the horizon  $N$ , since the KL divergence reward is non-decreasing. Figure 4 (left column) shows that our method converges to the horizon  $N = 3$ , achieving the analytical optimum, whereas naïve threshold rules stop prematurely and underperform.

For negative costs, Figure 4 (middle and right columns) illustrates two representative regimes. In the  $N = 3$  problem with  $c_k = -0.5$ , both vanilla and curriculum methods converge to the optimal early stopping at stage 1, consistent with the analytical solution. In the  $N = 4$  problem with  $c_k = -0.25$ , both methods achieve near-optimal final performance but exhibit different convergence behavior. The vanilla approach often underestimates the optimal stopping stage, becoming trapped below the analytical solution, whereas the curriculum method converges more reliably by exploring longer trajectories before settling at the correct stage. These results suggest that curriculum learning can improve the robustness of stopping-stage convergence when vanilla training tends to stop too early, although the effect is modest in this benchmark. The small discrepancy from the analytical solution in the  $N = 4$  case reflects a flat reward landscape, where stopping at stages 1–3 yields nearly indistinguishable rewards. Even in this setting, the PG method captures the relevant trade-offs, validating the proposed optimization approach. The remaining gap is attributed primarily to neural-network approximation and optimization choices, such as architecture and learning rate.

The distributional analysis in Figure 5 further confirms that the trained policy learns the analytical structure of the linear-Gaussian benchmark. The stopping-stage histogram shows that the policy predominantly terminates at stage 3 when experimental costs are absent. The design histogram shows that designs concentrate near the upper bound ( $\xi = 3$ ), where the signal-to-noise ratio is maximized. Together, these distributions indicate that the learned policy recovers both the optimal stopping behavior and the optimal design behavior in this benchmark.

## 4.2 One-dimensional nonlinear test problem

To further assess the method beyond the conjugate setting, we consider a one-dimensional nonlinear test problem. The forward model is

$$y_k = G(\theta, \xi_k) + \epsilon_k = \theta^3 \xi_k^2 + \theta \exp(-|0.2 - \xi_k|) + \epsilon_k, \quad \epsilon_k \sim \mathcal{N}(0, 0.03^2), \quad (27)$$

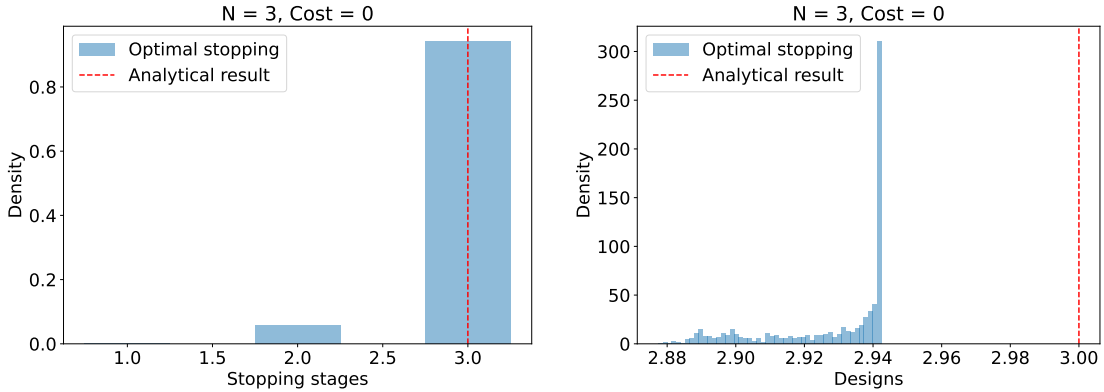


Figure 5: Distributional analysis of stopping stages (left) and experimental designs (right) for the linear-Gaussian benchmark with zero experimental cost ( $c_k = 0$ ).

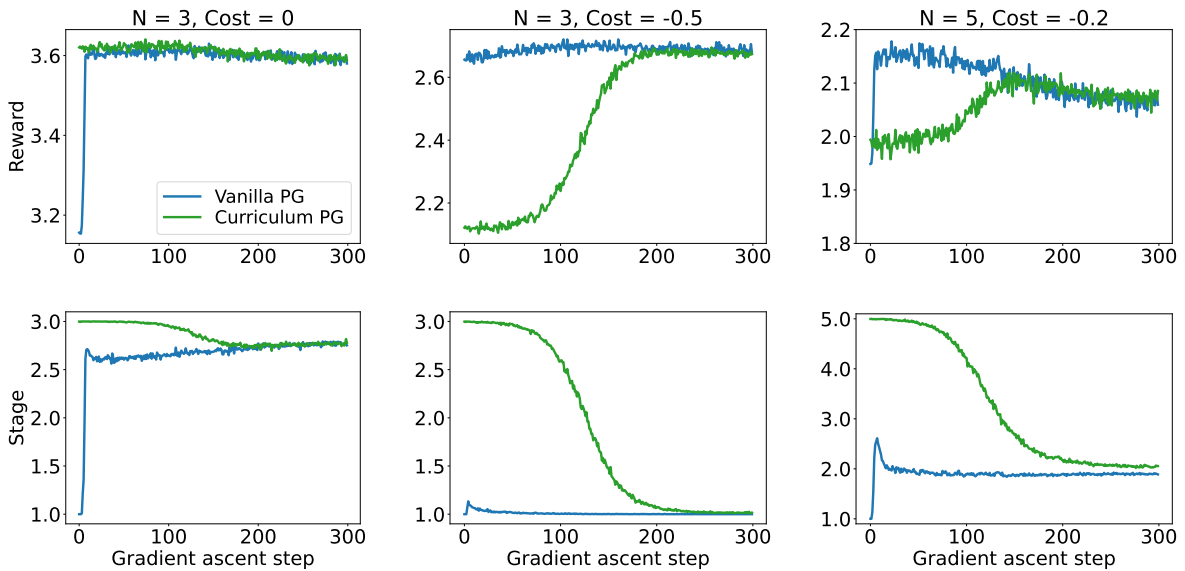


Figure 6: Training convergence of the one-dimensional nonlinear test problem. Top: average reward; bottom: average stopping stage. Columns correspond to different horizons  $N$  and experimental costs.

with prior  $\theta \sim \mathcal{U}(0, 1)$  and design constraint  $\xi_k \in [0, 1]$ . Unlike the preceding linear-Gaussian benchmark, this model is non-conjugate: the posterior is no longer Gaussian, and the expected continuation value depends on the realized observations through the full posterior shape. At the same time, the scalar parameter keeps posterior inference accurate and transparent, allowing us to isolate the effect of nonlinearity without adding unnecessary computational complexity.

Figure 6 summarizes three representative settings. With zero experimental cost and horizon  $N = 3$ , both vanilla PG and curriculum PG rapidly reach comparable rewards, and the learned stopping stage remains close to the terminal horizon. This is consistent with the nonnegative information-gain reward: in the absence of experimental cost, additional measurements are beneficial unless the posterior has already become sufficiently concentrated.

When a constant cost  $c_k = -0.5$  is imposed for the same horizon, the optimal behavior shifts toward early termination. Both methods converge to stopping after approximately one experiment, indicating that the first nonlinear observation already provides enough information to make further measurements unattractive relative to their cost. Curriculum PG initially explores longer trajectories, as intended, and then transitions to the same early-stopping regime once the stopping rule is fully activated.

For the longer horizon  $N = 5$  with moderate cost  $c_k = -0.2$ , both methods converge to similar final rewards and stopping stages, terminating around stage two. However, the training curves exhibit larger fluctuations. This behavior is consistent with a flatter reward landscape, where stopping at adjacent stages can yield nearly indistinguishable total rewards, analogous to the linear-Gaussian case with  $N = 4$  and  $c_k = -0.25$ . In the nonlinear problem, this trade-off is further complicated by sequential dependence, since each observation changes the posterior shape and hence the value of subsequent designs. As a result, small policy changes can shift trajectories among several nearly equivalent stopping behaviors, producing larger fluctuations even though both methods ultimately settle to comparable performance.

### 4.3 Contaminant Source Detection in a Convection-Diffusion Field

We next consider a sensor-movement problem for contaminant source detection, which exhibits stronger sequential dependence than the preceding examples. In the linear-Gaussian benchmark, the optimal design and stopping decisions are independent of the realized observations. In the one-dimensional nonlinear problem, observations affect future decisions through the updated posterior. Here, the dependence is stronger: the design variable is a sensor displacement, so the current sensor location is determined by the cumulative history of all previous designs, in addition to the information contained in past observations. Mobile sensors must therefore be strategically repositioned to localize an unknown pollution source, with each placement decision depending critically on both previous measurements and previously selected movements.

Contaminant transport is governed by a convection-diffusion PDE on a two-dimensional square domain  $[z_L, z_R]^2$ :

$$\frac{\partial G(z, t; \theta)}{\partial t} = \nabla^2 G - u(t) \cdot \nabla G + S(z, t; \theta), \quad z \in [z_L, z_R]^2, \quad t > 0 \quad (28)$$

where  $\theta = [\theta_x, \theta_y, \theta_h, \theta_s] \in \mathbb{R}^4$  parameterizes a Gaussian source

$$S(z, t; \theta) = \frac{\theta_s}{2\pi\theta_h^2} \exp\left(-\frac{(\theta_x - z_x)^2 + (\theta_y - z_y)^2}{2\theta_h^2}\right) \quad (29)$$

with location  $(\theta_x, \theta_y)$ , width  $\theta_h$ , and strength  $\theta_s$ , and  $u = [u_x, u_y] \in \mathbb{R}^2$  is a time-dependent convection velocity. A mobile sensor measures noisy concentrations

$$y_k = G(z = s_{k+1,p}, t_k; \theta) + \epsilon_k, \quad \epsilon_k \sim \mathcal{N}(0, \sigma_\epsilon^2), \quad (30)$$

where the design variable  $\xi_k$  represents sensor displacement,

$$s_{k+1,p} = s_{k,p} + \xi_k. \quad (31)$$

We consider  $N$  measurement opportunities at times  $t_k = k \cdot \Delta t$ ,  $k = 0, \dots, N - 1$ , with  $\Delta t = 5.0 \times 10^{-2}$ , and fix  $\theta_h = 0.05$ ,  $\theta_s = 2$ ,  $u_x = u_y = 10t/0.2$ , with prior  $\theta_x, \theta_y \sim \mathcal{U}(0, 1)$ .

The forward model (28) is solved numerically using a second-order finite volume method on a uniform grid with spatial resolution  $dz_x = dz_y = 0.01$ , together with a second-order fractional-step method for time integration using a timestep of  $dt = 5.0 \times 10^{-4}$ . Since repeated evaluations of the forward model are computationally expensive, we construct deep neural network (DNN) surrogate models for  $G(z, t_k; \theta)$  at each stage  $k$ . Each surrogate takes a 4-dimensional input  $(z, \theta)$  and maps it through five hidden layers containing 40, 80, 40, 20, and 10 neurons, respectively, to produce a scalar concentration output. The training dataset is generated from 2000 prior samples of  $\theta$ , restricted to the reachable domain and split 80%/20% for training and testing. Figure 7 compares concentration contours at four time points obtained from the finite volume solver (upper panel) and the DNN surrogate (lower panel). The two sets of contours are visually nearly indistinguishable, with test mean-squared errors on the order of  $10^{-6}$ . The surrogate models also provide a computational speedup of approximately  $10^5$  relative to the finite volume solver.

For zero cost ( $c_k = 0$ ), Figure 8 (left column) shows that both vanilla and curriculum learning converge successfully to the terminal horizon. Vanilla PG reaches the high-reward regime rapidly, while curriculum PG initially follows the forced-continuation schedule and then approaches a comparable reward. In this regime, continuation rewards dominate termination rewards, so even imperfect early designs provide sufficient information to favor continuing through the full horizon.

For negative costs, the training challenges identified in Section 3.2 become more evident. These cases reveal reward landscapes with multiple local optima associated with different stopping stages. The design variables are sensor movements rather than independent sensor locations, so each early movement changes the feasible locations and measurements available at later stages. If the critic underestimates the value of continuation early in training, the induced stopping rule truncates trajectories before the policy experiences informative later-stage moves. Those missing trajectories then reinforce the underestimated continuation value, creating an early-stopping local optimum.

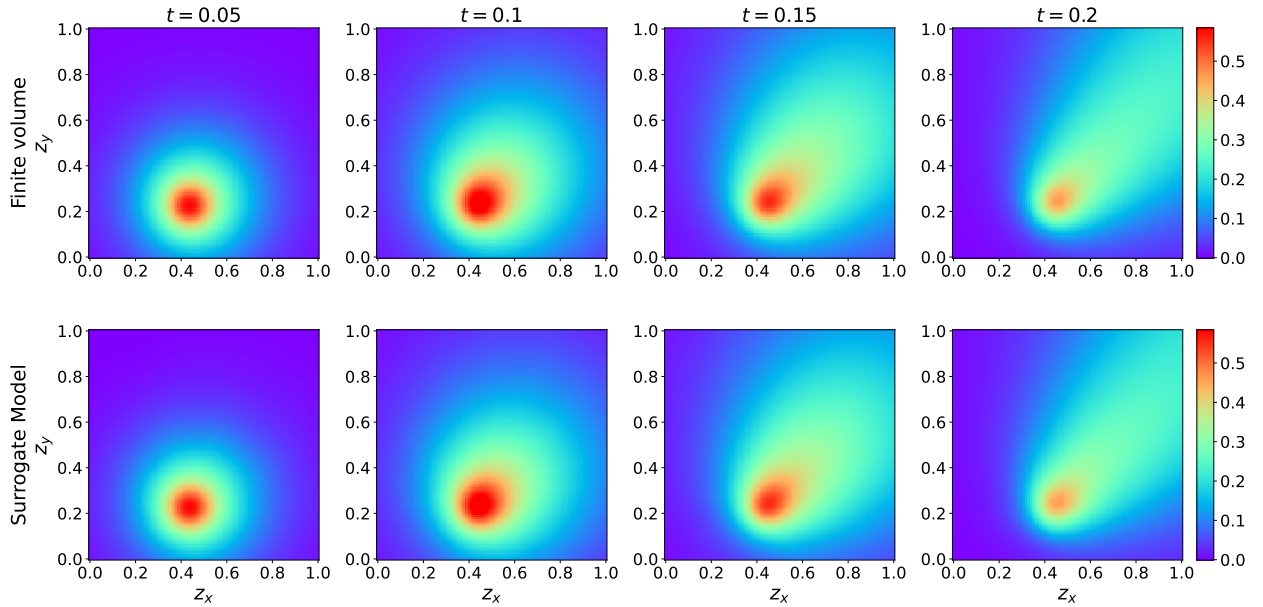


Figure 7: Comparison of the concentration field  $G$  at 4 time points with  $\theta_x = 0.43$  and  $\theta_y = 0.22$ , obtained using the finite volume (upper panel) and DNN surrogate (lower panel). The true solution is solved using finite volume in the wider computational domain  $[-1, 2]^2$  but displayed here in the region of interest  $[0, 1]^2$ .

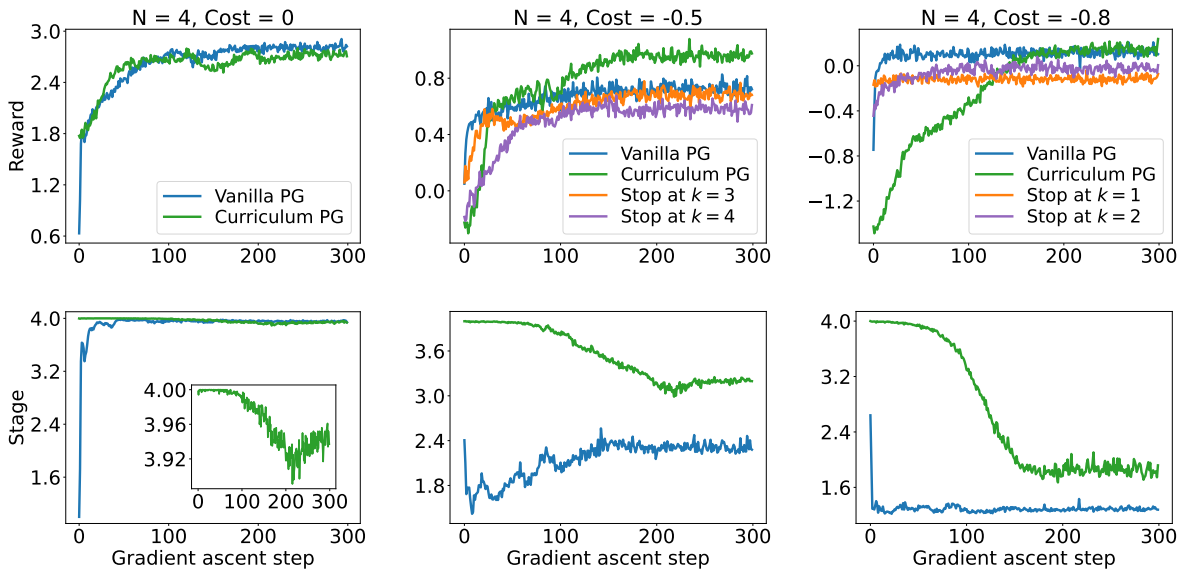


Figure 8: Training convergence of the convection-diffusion problem with horizon  $N = 4$ . Top: average reward; bottom: average stopping stage. Columns correspond to different experimental costs.

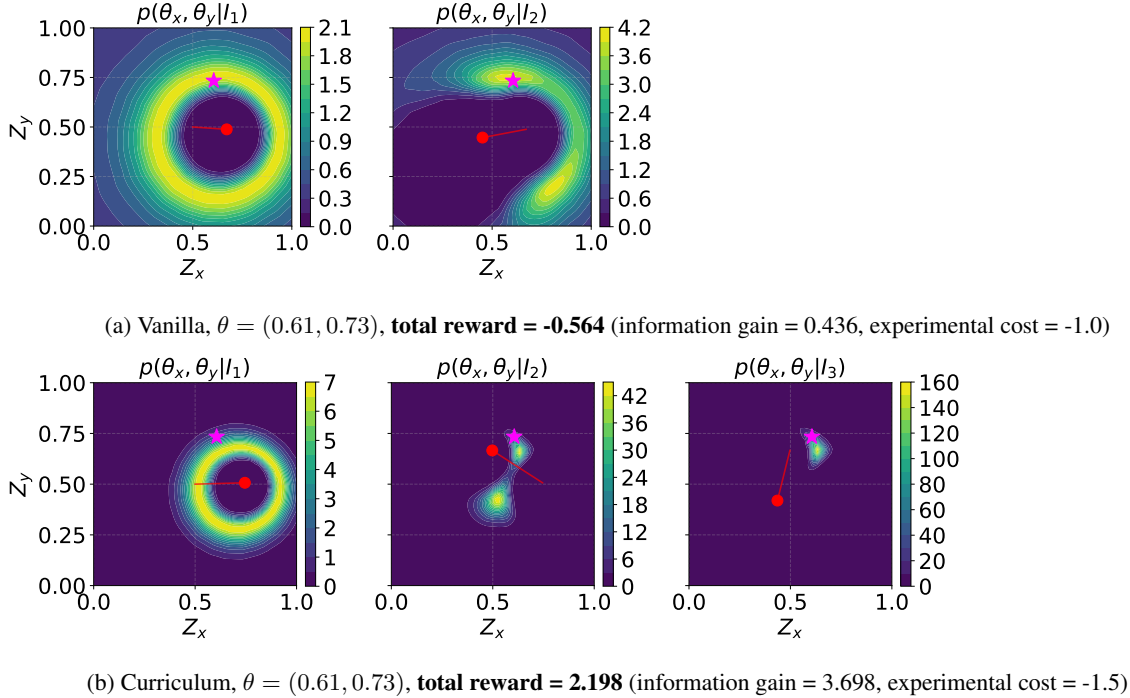


Figure 9: Episode instances for vanilla (upper) and curriculum (lower) policies in the  $c_k = -0.5$  scenario. Purple star: true source location; red dots: sensor positions; red lines: sensor movements; contours: posterior PDF.

With moderate cost ( $c_k = -0.5$ , middle column), the two local optima are clearly separated in reward. Vanilla PG converges to the earlier, lower-reward optimum, stopping at an average stage of approximately 2.4. In contrast, curriculum PG forces longer trajectories early in training, allowing the policy and critic to discover a later-stopping optimum with average stopping stage slightly above 3 and higher reward. This is the clearest case where the circular dependency produces a practical failure mode: vanilla PG becomes trapped in the smaller early-stopping optimum and misses the higher-reward solution discovered by curriculum PG.

At higher cost ( $c_k = -0.8$ , right column), the learning dynamics again indicate two local optima, as vanilla PG and curriculum PG converge to different average stopping stages. In this case, however, the two optima have similar objective values, so the final rewards are comparable. Vanilla PG reaches the earlier-stopping optimum, while curriculum PG converges to the later-stopping optimum because its training trajectories are forced to continue longer before the stopping rule is fully activated. Thus, curriculum learning helps avoid missing the global or higher-reward optimum by preserving long-horizon exploration before early stopping decisions are allowed to dominate training. In both negative-cost cases, the learned policies outperform fixed-stage stopping rules, indicating that the optimal stopping strategy in this problem is state-dependent rather than associated with a single fixed stopping stage.

Figure 9 presents representative episodes generated using the policies learned by the vanilla PG and curriculum PG methods for the case  $c_k = -0.5$ . Starting from the same initial condition, the two methods produce slightly different experimental designs at the initial stage, indicating that different stopping-learning strategies lead to different learned design policies. This further supports the circular dependency discussed earlier: premature stopping affects the learning of the design policy itself. The vanilla PG policy terminates after two experiments with a total reward of -0.564, while the curriculum-trained policy continues for three experiments and achieves a higher total reward of 2.198.

We further explore a more complex cost structure in the contaminant source detection problem with design-dependent experimental costs  $c_k = -3\|\xi_k\|$ , where longer sensor movements incur larger penalties. Figure 10 shows training convergence under this cost structure. Both vanilla and curriculum PG converge to similar rewards and stopping stages, with the average stopping stage approaching approximately 3.6–3.7. The design-dependent cost also changes the learned movement strategy. Figure 11 compares the spatial distribution of learned sensor movements under constant versus design-dependent costs across experimental stages. At stage  $k = 0$ , the fixed initial state makes the learned movement deterministic within each cost setting, although the selected initial movement differs between the two cost structures. Under the constant cost (upper panels), later-stage movements become more dispersed, especially for  $k = 2$  and  $k = 3$ , since movement length is not directly penalized. In contrast, under the design-dependent cost (lower panels),

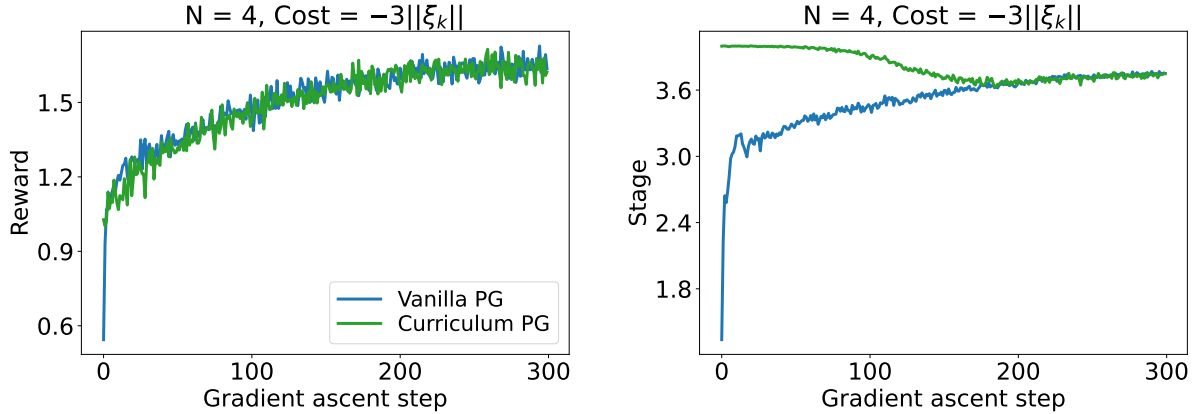


Figure 10: Training convergence of the convection-diffusion source detection problem with design-dependent costs  $c_k = -3\|\xi_k\|$ . Left: average reward; right: average stopping stage.

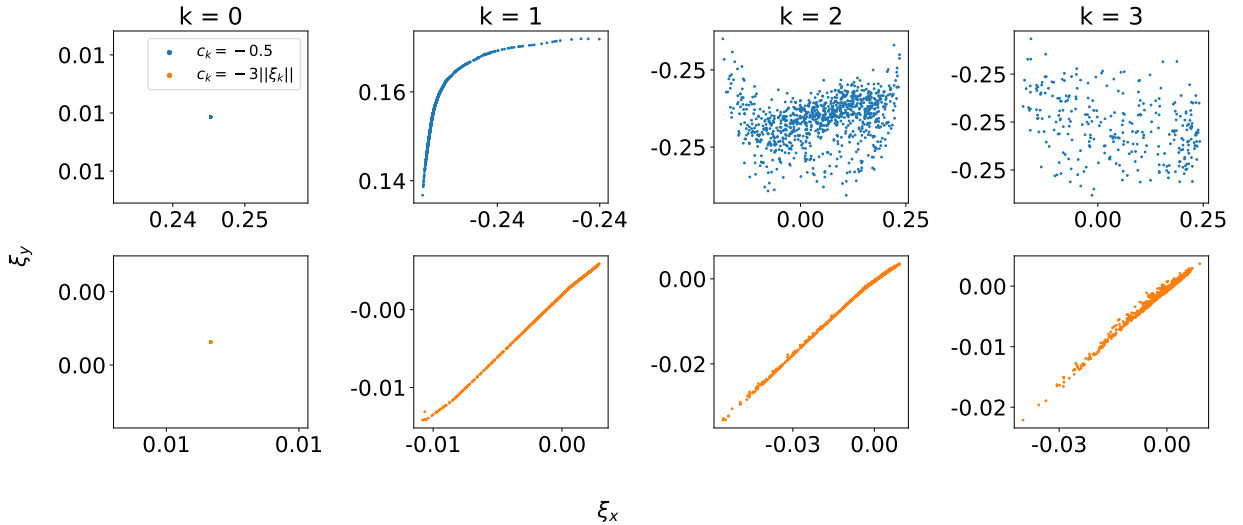


Figure 11: Comparison of learned sensor movement policies under constant versus design-dependent costs in the convection-diffusion source detection problem. Upper panels: constant cost  $c_k = -0.5$ . Lower panels: design-dependent cost  $c_k = -3\|\xi_k\|$ .

the learned movements concentrate along a narrow trajectory with much smaller magnitudes, reflecting a policy that balances information acquisition against the linear movement penalty. This adaptive behavior demonstrates that our framework successfully incorporates spatially varying costs into the joint design and stopping optimization.

These results demonstrate that the proposed framework can accommodate complex, design-dependent cost structures. They also show that the benefit of curriculum learning depends on the interaction between cost, stopping, and sequential design dependence: in this design-dependent-cost setting, vanilla and curriculum training converge to similar stopping stages and rewards, while in regimes where premature stopping suppresses later-stage exploration, curriculum learning can provide a clear advantage.

Overall, these results demonstrate that strong sequential dependence combined with cost-sensitive stopping can destabilize joint optimization, trapping vanilla PG in suboptimal early-stopping policies. Curriculum learning mitigates this effect by preserving longer training trajectories before adaptive stopping dominates, with the clearest gains appearing when premature stopping would otherwise suppress later-stage exploration. To illustrate the role of the curriculum schedule, we compared several common choices for the stopping probability  $p_{\text{stop}}(\ell)$  in Figure 12, including linear, exponential, and sigmoid increases. As shown in Figure 13, these schedules behave similarly on relatively simple

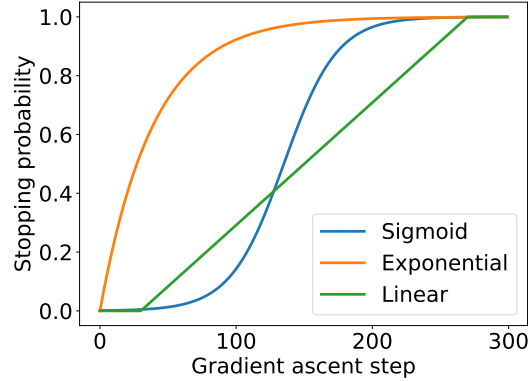


Figure 12: Examples of stopping probability schedules for curriculum PG over 300 training iterations.

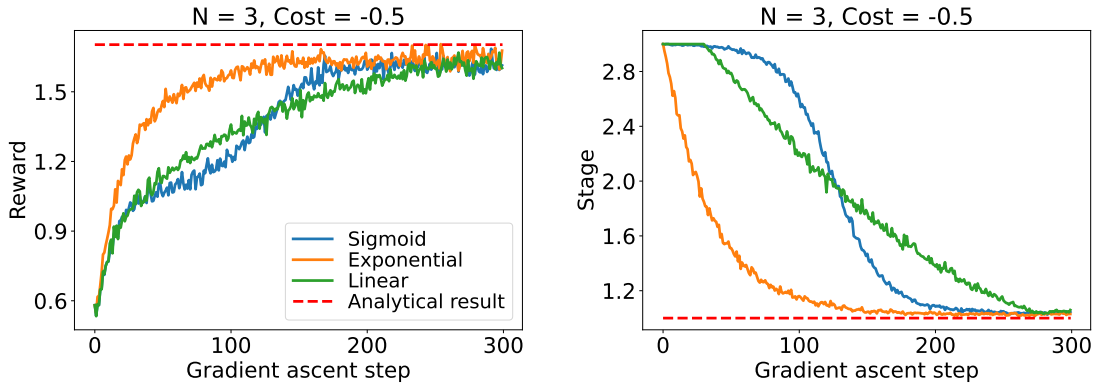


Figure 13: Comparison of different curriculum schedules on the Linear-Gaussian benchmark. Left: average reward; right: average stopping stage.

problems such as the linear-Gaussian benchmark: all converge to the optimal policy, differing mainly in convergence patterns and speed. However, for more complex or long-horizon tasks such as the contaminant source detection problem, the choice of schedule becomes critical. As shown in Figure 14, a fast exponential schedule leads to insufficient exploration during early training, resulting in training instability and convergence to a suboptimal policy. In contrast, sigmoid and linear schedules with slower progression rates ensure adequate full-horizon exploration in early stages, leading to stable training and superior final performance. These results suggest that practitioners should tune the curriculum schedule based on problem complexity: simple problems tolerate aggressive schedules, while complex tasks benefit from gradual transitions that maintain exploration before allowing the optimal stopping rule to dominate training dynamics.

## 5 Conclusion

This paper addressed the problem of deciding when to terminate a sequential Bayesian experimental design campaign. The central idea is to treat stopping as part of the sequential decision problem rather than as a fixed threshold rule. This leads to an interpretable optimal stopping criterion: experimentation should continue only when the expected continuation value exceeds the immediate terminal reward.

The resulting optimization problem is challenging because the design policy, continuation value, and stopping boundary are mutually dependent. We developed a policy gradient method that exploits the value-based stopping structure and augments it with curriculum learning, gradually moving from forced continuation to adaptive stopping during training. Across a linear-Gaussian benchmark, a nonlinear non-conjugate test problem, and a convection-diffusion source detection problem, the method learned effective design-stopping policies. The experiments show that curriculum

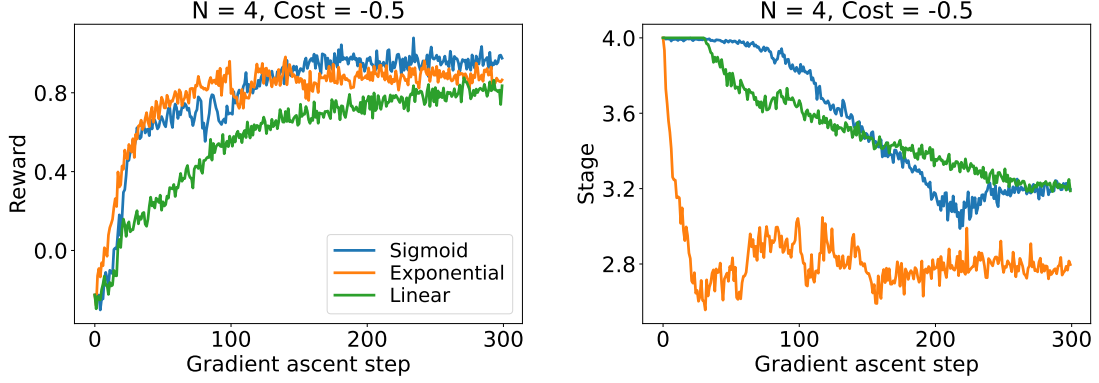


Figure 14: Comparison of different curriculum schedules on the convection-diffusion source detection problem. Left: average reward; right: average stopping stage.

learning is most valuable when premature stopping prevents the policy from observing informative later-stage trajectories, as in the movement-constrained source detection problem with moderate experimental cost.

Several limitations motivate future work. First, evaluating terminal rewards at each decision stage can be expensive when posterior updates are costly or high dimensional. Second, alternative approaches that directly parameterize the stopping policy, without relying on the optimal stopping theorem (Theorem 3.1), may avoid circular dependencies and simplify training, albeit potentially at the expense of slower convergence or weaker theoretical guarantees. Finally, this paper focuses on information gain for parameter inference, but the same framework can accommodate goal-oriented utilities, such as improving predictions of future outcomes as in related work by [Kleinegesse and Gutmann \(2021\)](#). These extensions would broaden the applicability of optimal stopping to autonomous experimental systems with richer scientific and engineering objectives.

Overall, this work advances the development of autonomous experimental systems by enabling intelligent, resource-aware stopping decisions, improving the efficiency and robustness of sequential Bayesian experimental design.

## A Appendix

### A.1 Proof of Theorem 3.1

*Proof of Theorem 3.1.* For a given design policy  $\pi$ , consider the V-function under any stopping policy  $\psi'$  different from  $\psi$ :

$$\begin{aligned} V_N^{\pi, \psi'}(s_N) &= r_T(s_N) \\ V_k^{\pi, \psi'}(s_k) &= \begin{cases} r_T^S(s_k), & \varphi'_k(s_k) = 1, \\ \mathbb{E}_{y_k|\pi, s_k} \left[ r_k^C(s_k, \mu_k(s_k), y_k) + V_{k+1}^{\pi, \psi'}(\mathcal{F}_k(s_k, \mu_k(s_k), y_k)) \right], & \text{otherwise.} \end{cases} \end{aligned} \quad (32)$$

Note that at the terminal stage,  $V_N^{\pi, \psi}(s_N) = r_T(s_N) = V_N^{\pi, \psi'}(s_N)$ . V-function under the optimal stopping policy  $\psi$  satisfies:

$$V_k^{\pi, \psi}(s_k) = \max \left\{ r_T^S(s_k), \mathbb{E}_{y_k|\pi, s_k} \left[ r_k^C(s_k, \mu_k(s_k), y_k) + V_{k+1}^{\pi, \psi}(\mathcal{F}_k(s_k, \mu_k(s_k), y_k)) \right] \right\}. \quad (33)$$

**Base case ( $k = N - 1$ ).** If  $\varphi'_{N-1}(s_{N-1}) = 1$ , then

$$\begin{aligned} V_{N-1}^{\pi, \psi'}(s_{N-1}) &= r_T^S(s_{N-1}) \\ &\leq \max \left\{ r_T^S(s_{N-1}), \mathbb{E}_{y_{N-1}|\pi, s_{N-1}} \left[ r_{N-1}^C(s_{N-1}, \mu_{N-1}(s_{N-1}), y_{N-1}) \right. \right. \\ &\quad \left. \left. + V_N^{\pi, \psi}(\mathcal{F}_{N-1}(s_{N-1}, \mu_{N-1}(s_{N-1}), y_{N-1})) \right] \right\} \\ &= V_{N-1}^{\pi, \psi}(s_{N-1}). \end{aligned} \quad (34)$$

If  $\varphi'_{N-1}(s_{N-1}) = 0$ , then

$$\begin{aligned}
V_{N-1}^{\pi, \psi'}(s_{N-1}) &= \mathbb{E}_{y_{N-1}|\pi, s_{N-1}} \left[ r_{N-1}^C(s_{N-1}, \mu_{N-1}(s_{N-1}), y_{N-1}) + V_N^{\pi, \psi'}(\mathcal{F}_{N-1}(s_{N-1}, \mu_{N-1}(s_{N-1}), y_{N-1})) \right] \\
&= \mathbb{E}_{y_{N-1}|\pi, s_{N-1}} \left[ r_{N-1}^C(s_{N-1}, \mu_{N-1}(s_{N-1}), y_{N-1}) + V_N^{\pi, \psi}(\mathcal{F}_{N-1}(s_{N-1}, \mu_{N-1}(s_{N-1}), y_{N-1})) \right] \\
&\leq \max \left\{ r_T^S(s_{N-1}), \mathbb{E}_{y_{N-1}|\pi, s_{N-1}} \left[ r_{N-1}^C(s_{N-1}, \mu_{N-1}(s_{N-1}), y_{N-1}) \right. \right. \\
&\quad \left. \left. + V_N^{\pi, \psi}(\mathcal{F}_{N-1}(s_{N-1}, \mu_{N-1}(s_{N-1}), y_{N-1})) \right] \right\} \\
&= V_{N-1}^{\pi, \psi}(s_{N-1}).
\end{aligned} \tag{35}$$

Hence,  $V_{N-1}^{\pi, \psi}(s_{N-1}) \geq V_{N-1}^{\pi, \psi'}(s_{N-1})$ .

**Inductive step.** Suppose  $V_{k+1}^{\pi, \psi}(s_{k+1}) \geq V_{k+1}^{\pi, \psi'}(s_{k+1})$ . Then

$$\begin{aligned}
V_k^{\pi, \psi}(s_k) &= \max \left\{ r_T^S(s_k), \mathbb{E}_{y_k|\pi, s_k} \left[ r_k^C(s_k, \mu_k(s_k), y_k) + V_{k+1}^{\pi, \psi}(\mathcal{F}_k(s_k, \mu_k(s_k), y_k)) \right] \right\} \\
&\geq \max \left\{ r_T^S(s_k), \mathbb{E}_{y_k|\pi, s_k} \left[ r_k^C(s_k, \mu_k(s_k), y_k) + V_{k+1}^{\pi, \psi'}(\mathcal{F}_k(s_k, \mu_k(s_k), y_k)) \right] \right\} \\
&\geq V_k^{\pi, \psi'}(s_k).
\end{aligned} \tag{36}$$

By induction,  $V_k^{\pi, \psi}(s_k) \geq V_k^{\pi, \psi'}(s_k)$  for all  $k = 0, \dots, N-1$ . In particular,  $V_0^{\pi, \psi}(s_0) \geq V_0^{\pi, \psi'}(s_0)$ , which proves that the stopping policy in Theorem 3.1 is optimal.  $\square$

## A.2 Proof of Theorem 3.2

*Proof of Theorem 3.2.* We first prove the stopping sets are equivalent under two formulations. For convenience, we omit the notation of design policy  $\pi$  and stopping policy  $\psi$ , but distinguish them using superscripts of *incr* and *term* respectively. The policy dependence in the expectations is also omitted for notational consistency. We first prove the following relationship between value functions:

$$V_k^{incr}(s_k) = V_k^{term}(s_k) - \left[ D_{\text{KL}}(p_{\theta|I_k} \| p_{\theta|I_0}) + \sum_{i=0}^{k-1} c_i(\xi_i) \right], k = 0, \dots, N. \tag{37}$$

**Base case ( $k = N$ ).** For the terminal formulation,

$$V_N^{term}(s_N) = r_T(s_N) = D_{\text{KL}}(p_{\theta|I_N} \| p_{\theta|I_0}) + \sum_{i=0}^{N-1} c_i(\xi_i); \tag{38}$$

for the incremental formulation,

$$V_N^{incr}(s_N) = r_T(s_N) = 0. \tag{39}$$

Therefore

$$V_N^{incr}(s_N) = V_N^{term}(s_N) - \left[ D_{\text{KL}}(p_{\theta|I_N} \| p_{\theta|I_0}) + \sum_{i=0}^{N-1} c_i(\xi_i) \right]. \tag{40}$$

**Inductive step.** Suppose

$$V_{k+1}^{incr}(s_{k+1}) = V_{k+1}^{term}(s_{k+1}) - \left[ D_{\text{KL}}(p_{\theta|I_{k+1}} \| p_{\theta|I_0}) + \sum_{i=0}^k c_i(\xi_i) \right]. \tag{41}$$

Then at stage  $k$ , for the terminal formulation,

$$V_k^{term}(s_k) = \max \left\{ D_{\text{KL}}(p_{\theta|I_k} \| p_{\theta|I_0}) + \sum_{i=0}^{k-1} c_i(\xi_i), \mathbb{E}_{y_k} [V_{k+1}^{term}(s_{k+1})] \right\}; \tag{42}$$

for the incremental formulation,

$$\begin{aligned}
& V_k^{incr}(s_k) \\
&= \max \left\{ 0, \mathbb{E}_{y_k} \left[ D_{\text{KL}}(p_{\theta|I_{k+1}} \| p_{\theta|I_k}) + c_k(\xi_k) + V_{k+1}^{incr}(s_{k+1}) \right] \right\} \\
&= \max \left\{ 0, \mathbb{E}_{y_k} \left[ D_{\text{KL}}(p_{\theta|I_{k+1}} \| p_{\theta|I_k}) + c_k(\xi_k) + V_{k+1}^{term}(s_{k+1}) - D_{\text{KL}}(p_{\theta|I_{k+1}} \| p_{\theta|I_0}) - \sum_{i=0}^k c_i(\xi_i) \right] \right\} \\
&= \max \left\{ 0, \mathbb{E}_{y_k} \left[ V_{k+1}^{term}(s_{k+1}) - D_{\text{KL}}(p_{\theta|I_k} \| p_{\theta|I_0}) - \sum_{i=0}^{k-1} c_i(\xi_i) \right] \right\} \\
&= \max \left\{ D_{\text{KL}}(p_{\theta|I_k} \| p_{\theta|I_0}) + \sum_{i=0}^{k-1} c_i(\xi_i), \mathbb{E}_{y_k} \left[ V_{k+1}^{term}(s_{k+1}) \right] \right\} - \left[ D_{\text{KL}}(p_{\theta|I_k} \| p_{\theta|I_0}) + \sum_{i=0}^{k-1} c_i(\xi_i) \right] \\
&= V_k^{term}(s_k) - \left[ D_{\text{KL}}(p_{\theta|I_k} \| p_{\theta|I_0}) + \sum_{i=0}^{k-1} c_i(\xi_i) \right]. \tag{43}
\end{aligned}$$

By induction, (37) is proved. Using this relationship, we examine the stopping sets. The terminal formulation stopping sets are:

$$\mathcal{T}_k^{term} = \left\{ s_k \mid D_{\text{KL}}(p_{\theta|I_k} \| p_{\theta|I_0}) + \sum_{i=0}^{k-1} c_i(\xi_i) \geq \mathbb{E}_{y_k} \left[ V_{k+1}^{term}(s_{k+1}) \right] \right\}; \tag{44}$$

the incremental stopping sets are:

$$\begin{aligned}
\mathcal{T}_k^{incr} &= \{ s_k \mid 0 \geq \mathbb{E}_{y_k} [r_k^C(s_k, \xi_k, y_k) + V_{k+1}^{incr}(s_{k+1})] \} \\
&= \{ s_k \mid 0 \geq \mathbb{E}_{y_k} [D_{\text{KL}}(p_{\theta|I_{k+1}} \| p_{\theta|I_k}) + c_k(\xi_k) + V_{k+1}^{incr}(s_{k+1})] \} \\
&= \left\{ s_k \mid 0 \geq \mathbb{E}_{y_k} \left[ V_{k+1}^{term}(s_{k+1}) - D_{\text{KL}}(p_{\theta|I_k} \| p_{\theta|I_0}) - \sum_{i=0}^{k-1} c_i(\xi_i) \right] \right\} \\
&= \mathcal{T}_k^{term}. \tag{45}
\end{aligned}$$

Therefore, the stopping sets are equivalent in both formulations. In particular, the optimization objective is

$$U(\pi, \psi) = V_0^{incr}(s_0) = V_0^{term}(s_0), \tag{46}$$

which further proves the equivalence of the optimization problem.  $\square$

### A.3 Proof of Theorem 3.3

To simplify notation, below we omit the subscript on  $w$  and shorten  $\mu_{k,w_k}(s_k)$  to  $\mu_{k,w}(s_k)$ , with the understanding that  $w$  takes the same subscript as the  $\mu$  function. We also suppress explicit conditioning in expectations whenever the underlying measure is clear from context. Throughout the proof, we impose the following regularity assumptions, which are standard in sequential decision problems with differentiable policies.

**Assumption A.1.** (i) The observation noise  $\varepsilon_k$  admits a density with respect to Lebesgue measure. (ii) The design policy  $\mu_{k,w}(s_k)$  is differentiable in  $w$  for almost every  $s_k$ . (iii) The observation density  $p(y_k \mid s_k, \xi_k)$  and the forward map  $\mathcal{F}_k(s_k, \xi_k, y_k)$  are differentiable in  $\xi_k$ . (iv) The derivatives in (iii) and the policy gradient  $\nabla_w \mu_{k,w}$  are bounded.

*Proof of Theorem 3.3.* The gradient of the expected utility can be expressed in terms of the value function:

$$\nabla_w U(w) = \nabla_w V_0^{\pi_w, \psi_w}(s_0). \tag{47}$$

By denoting the V-function as

$$\begin{aligned}
V_k^{\pi_w, \psi_w}(s_k) &= \mathbf{1}_{s_k \in \mathcal{T}_{k,w}} r_T^S(s_k) + (1 - \mathbf{1}_{s_k \in \mathcal{T}_{k,w}}) \mathbb{E}_{y_k} \left[ r_k^C(s_k, \mu_{k,w}(s_k), y_k) + V_{k+1}^{\pi_w, \psi_w}(\mathcal{F}_k(s_k, \mu_{k,w}(s_k), y_k)) \right] \\
&= \mathbf{1}_{s_k \in \mathcal{T}_{k,w}} r_T^S(s_k) + (1 - \mathbf{1}_{s_k \in \mathcal{T}_{k,w}}) Q_k(s_k, w) \tag{48}
\end{aligned}$$

where  $Q_k(s_k, w) = Q_k^{\pi_w, \psi_w}(s_k, \mu_{k,w}(s_k)) = \mathbb{E}_{y_k} \left[ r_k^C(s_k, \mu_{k,w}(s_k), y_k) + V_{k+1}^{\pi_w, \psi_w}(\mathcal{F}_k(s_k, \mu_{k,w}(s_k), y_k)) \right]$ , differentiating  $V_k^{\pi_w, \psi_w}(s_k)$  with respect to  $w$  yields

$$\nabla_w V_k^{\pi_w, \psi_w}(s_k) = \nabla_w \mathbf{1}_{s_k \in \mathcal{T}_{k,w}} r_T^S(s_k) - \nabla_w \mathbf{1}_{s_k \in \mathcal{T}_{k,w}} Q_k(s_k, w) + (1 - \mathbf{1}_{s_k \in \mathcal{T}_{k,w}}) \nabla_w Q_k(s_k, w)$$

$$= \nabla_w \mathbf{1}_{s_k \in \mathcal{T}_{k,w}} [r_T^S(s_k) - Q_k(s_k, w)] + \mathbf{1}_{s_k \notin \mathcal{T}_{k,w}} \nabla_w Q_k(s_k, w). \quad (49)$$

The first term in (49) is related to the gradient of an indicator function. To compute this, we define the boundary of the stopping set  $\mathcal{T}_{k,w}$  as

$$\partial \mathcal{T}_{k,w} = \{s_k \mid h(s_k, w) := r_T^S(s_k) - Q_k(s_k, w) = 0\}, \quad (50)$$

and correspondingly  $\mathcal{T}_{k,w} = \{s_k \mid h(s_k, w) > 0\}$ ,  $\mathcal{T}_{k,w}^c = \{s_k \mid h(s_k, w) \leq 0\}$ . Since the indicator function changes value only on this boundary, its gradient can be represented in distributional form using a Dirac delta supported on  $\partial \mathcal{T}_{k,w}$ :

$$\nabla_w \mathbf{1}_{s_k \in \mathcal{T}_{k,w}} = \delta(h(s_k, w)) \nabla_w h(s_k, w). \quad (51)$$

The first term in (49) is then reduced to  $h(s_k, w) \delta(h(s_k, w)) \nabla_w h(s_k, w)$ . Using the identity  $x \delta(x) \equiv 0$ , this boundary contribution vanishes. For the second term in (49),

$$\begin{aligned} \nabla_w Q_k(s_k, w) &= \nabla_w \mathbb{E}_{y_k} \left[ r_k^C(s_k, \mu_{k,w}(s_k), y_k) + V_{k+1}^{\pi_w, \psi_w}(\mathcal{F}_k(s_k, \mu_{k,w}(s_k), y_k)) \right] \\ &= \nabla_w \mathbb{E}_{y_k} \left[ r_k^C(s_k, \mu_{k,w}(s_k), y_k) \right] + \nabla_w \mathbb{E}_{y_k} \left[ V_{k+1}^{\pi_w, \psi_w}(\mathcal{F}_k(s_k, \mu_{k,w}(s_k), y_k)) \right], \end{aligned} \quad (52)$$

the latter term requires differentiating an expectation whose domain depends implicitly on  $w$  through the stopping region. This can be handled using the Leibniz rule for parameter-dependent integration domains, yielding both an interior gradient term and a boundary term proportional to the normal velocity of the moving boundary (see (Reed, Simon, Simon and Simon, 1972; Evans, 2022)).

$$\begin{aligned} & \nabla_w \mathbb{E}_{y_k} \left[ V_{k+1}^{\pi_w, \psi_w}(\mathcal{F}_k(s_k, \mu_{k,w}(s_k), y_k)) \right] \\ &= \nabla_w \int_{s_{k+1}} p(s_{k+1} | s_k, \mu_{k,w}(s_k)) V_{k+1}^{\pi_w, \psi_w}(s_{k+1}) ds_{k+1} \\ &= \nabla_w \left[ \int_{\mathcal{T}_{k+1,w}} r_T^S(s_{k+1}) p(s_{k+1} | s_k, \mu_{k,w}(s_k)) ds_{k+1} + \int_{\mathcal{T}_{k+1,w}^c} Q_{k+1}(s_{k+1}, w) p(s_{k+1} | s_k, \mu_{k,w}(s_k)) ds_{k+1} \right] \\ &= \int_{\mathcal{T}_{k+1,w}} \nabla_w \left[ r_T^S(s_{k+1}) p(s_{k+1} | s_k, \mu_{k,w}(s_k)) \right] ds_{k+1} + \int_{\partial \mathcal{T}_{k+1,w}} r_T^S(s_{k+1}) p(s_{k+1} | s_k, \mu_{k,w}(s_k)) \frac{\nabla_w h(s_{k+1}, w)}{|\nabla_{s_{k+1}} h(s_{k+1}, w)|} ds_{k+1} \\ & \quad + \int_{\mathcal{T}_{k+1,w}^c} \nabla_w [Q_{k+1}(s_{k+1}, w) p(s_{k+1} | s_k, \mu_{k,w}(s_k))] ds_{k+1} \\ & \quad - \int_{\partial \mathcal{T}_{k+1,w}} Q_{k+1}(s_{k+1}, w) p(s_{k+1} | s_k, \mu_{k,w}(s_k)) \frac{\nabla_w h(s_{k+1}, w)}{|\nabla_{s_{k+1}} h(s_{k+1}, w)|} ds_{k+1} \\ &= \int_{\mathcal{T}_{k+1,w}} \left[ p(s_{k+1} | s_k, \mu_{k,w}(s_k)) \nabla_w r_T^S(s_{k+1}) + \nabla_w \mu_{k,w}(s_k) \nabla_{\xi_k} p(s_{k+1} | s_k, \xi_k) \Big|_{\xi_k = \mu_{k,w}(s_k)} r_T^S(s_{k+1}) \right] ds_{k+1} \\ & \quad + \int_{\mathcal{T}_{k+1,w}^c} \left[ p(s_{k+1} | s_k, \mu_{k,w}(s_k)) \nabla_w Q_{k+1}(s_{k+1}, w) + \nabla_w \mu_{k,w}(s_k) \nabla_{\xi_k} p(s_{k+1} | s_k, \xi_k) \Big|_{\xi_k = \mu_{k,w}(s_k)} Q_{k+1}(s_{k+1}, w) \right] ds_{k+1} \\ & \quad + \int_{\partial \mathcal{T}_{k+1,w}} \left[ r_T^S(s_{k+1}) - Q_{k+1}(s_{k+1}, w) \right] p(s_{k+1} | s_k, \mu_{k,w}(s_k)) \frac{\nabla_w h(s_{k+1}, w)}{|\nabla_{s_{k+1}} h(s_{k+1}, w)|} ds_{k+1} \\ &= \int_{s_{k+1}} \left[ p(s_{k+1} | s_k, \mu_{k,w}(s_k)) \nabla_w V_{k+1}^{\pi_w, \psi_w}(s_{k+1}) + \nabla_w \mu_{k,w}(s_k) \nabla_{\xi_k} p(s_{k+1} | s_k, \xi_k) \Big|_{\xi_k = \mu_{k,w}(s_k)} V_{k+1}^{\pi_w, \psi_w}(s_{k+1}) \right] ds_{k+1} \\ &= \mathbb{E}_{y_k} \left[ \nabla_w V_{k+1}^{\pi_w, \psi_w}(\mathcal{F}_k(s_k, \mu_{k,w}(s_k), y_k)) \right], \end{aligned} \quad (53)$$

where the contribution of the boundary term vanishes since  $r_T^S(s_{k+1}) - Q_{k+1}(s_{k+1}, w) = 0$  on  $\partial \mathcal{T}_{k+1,w}$ . Combining the above identities yields

$$\begin{aligned} & \nabla_w Q_k(s_k, w) \\ &= \int_{y_k} \nabla_w \mu_{k,w}(s_k) \nabla_{\xi_k} \left[ p(y_k | s_k, \xi_k) r_k^C(s_k, \xi_k, y_k) \right] \Big|_{\xi_k = \mu_{k,w}(s_k)} dy_k \\ & \quad + \int_{s_{k+1}} \left[ p(s_{k+1} | s_k, \mu_{k,w}(s_k)) \nabla_w V_{k+1}^{\pi_w, \psi_w}(s_{k+1}) + \nabla_w \mu_{k,w}(s_k) \nabla_{\xi_k} p(s_{k+1} | s_k, \xi_k) \Big|_{\xi_k = \mu_{k,w}(s_k)} V_{k+1}^{\pi_w, \psi_w}(s_{k+1}) \right] ds_{k+1} \end{aligned}$$

$$\begin{aligned}
&= \nabla_w \mu_{k,w}(s_k) \nabla_{\xi_k} \left[ \int_{y_k} p(y_k | s_k, \xi_k) r_k^C(s_k, \xi_k, y_k) dy_k + \int_{s_{k+1}} p(s_{k+1} | s_k, \xi_k) V_{k+1}^{\pi_w, \psi_w}(s_{k+1}) ds_{k+1} \right] \Big|_{\xi_k = \mu_{k,w}(s_k)} \\
&\quad + \int_{s_{k+1}} p(s_{k+1} | s_k, \mu_{k,w}(s_k)) \nabla_w V_{k+1}^{\pi_w, \psi_w}(s_{k+1}) ds_{k+1} \\
&= \nabla_w \mu_{k,w}(s_k) \nabla_{\xi_k} Q_k^{\pi_w, \psi_w}(s_k, \xi_k) \Big|_{\xi_k = \mu_{k,w}(s_k)} + \int_{s_{k+1}} p(s_k \rightarrow s_{k+1} | \pi_w, \psi_w) \nabla_w V_{k+1}^{\pi_w, \psi_w}(s_{k+1}) ds_{k+1}. \tag{54}
\end{aligned}$$

Finally (49) gives us

$$\begin{aligned}
\nabla_w V_k^{\pi_w, \psi_w}(s_k) &= \mathbf{1}_{s_k \notin \mathcal{T}_{k,w}} \nabla_w \mu_{k,w}(s_k) \nabla_{\xi_k} Q_k^{\pi_w, \psi_w}(s_k, \xi_k) \Big|_{\xi_k = \mu_{k,w}(s_k)} \\
&\quad + \mathbf{1}_{s_k \in \mathcal{T}_{k,w}} \int_{s_{k+1}} p(s_k \rightarrow s_{k+1} | \pi_w, \psi_w) \nabla_w V_{k+1}^{\pi_w, \psi_w}(s_{k+1}) ds_{k+1}. \tag{55}
\end{aligned}$$

Applying the recursive (55) to itself repeatedly, we obtain

$$\begin{aligned}
&\nabla_w V_k^{\pi_w, \psi_w}(s_k) \\
&= \mathbf{1}_{s_k \notin \mathcal{T}_{k,w}} \nabla_w \mu_{k,w}(s_k) \nabla_{\xi_k} Q_k^{\pi_w, \psi_w}(s_k, \xi_k) \Big|_{\xi_k = \mu_{k,w}(s_k)} \\
&\quad + \mathbf{1}_{s_k \in \mathcal{T}_{k,w}} \int_{s_{k+1}} p(s_k \rightarrow s_{k+1} | \pi_w, \psi_w) \\
&\quad \quad \cdot \mathbf{1}_{s_{k+1} \notin \mathcal{T}_{k+1,w}} \nabla_w \mu_{k+1,w}(s_{k+1}) \nabla_{\xi_{k+1}} Q_{k+1}^{\pi_w, \psi_w}(s_{k+1}, \xi_{k+1}) \Big|_{\xi_{k+1} = \mu_{k+1,w}(s_{k+1})} ds_{k+1} \\
&\quad + \mathbf{1}_{s_k \in \mathcal{T}_{k,w}} \int_{s_{k+1}} p(s_k \rightarrow s_{k+1} | \pi_w, \psi_w) \mathbf{1}_{s_{k+1} \in \mathcal{T}_{k+1,w}} \\
&\quad \quad \cdot \int_{s_{k+2}} p(s_{k+1} \rightarrow s_{k+2} | \pi_w, \psi_w) \nabla_w V_{k+2}^{\pi_w, \psi_w}(s_{k+2}) ds_{k+2} ds_{k+1} \\
&= \prod_{j=k}^k \mathbf{1}_{s_j \notin \mathcal{T}_{j,w}} \nabla_w \mu_{k,w}(s_k) \nabla_{\xi_k} Q_k^{\pi_w, \psi_w}(s_k, \xi_k) \Big|_{\xi_k = \mu_{k,w}(s_k)} \\
&\quad + \int_{s_{k+1}} p(s_k \rightarrow s_{k+1} | \pi_w, \psi_w) \cdot \prod_{j=k}^{k+1} \mathbf{1}_{s_j \notin \mathcal{T}_{j,w}} \nabla_w \mu_{k+1,w}(s_{k+1}) \nabla_{\xi_{k+1}} Q_{k+1}^{\pi_w, \psi_w}(s_{k+1}, \xi_{k+1}) \Big|_{\xi_{k+1} = \mu_{k+1,w}(s_{k+1})} ds_{k+1} \\
&\quad + \int_{s_{k+2}} p(s_k \rightarrow s_{k+2} | \pi_w, \psi_w) \prod_{j=k}^{k+1} \mathbf{1}_{s_j \notin \mathcal{T}_{j,w}} \nabla_w V_{k+2}^{\pi_w, \psi_w}(s_{k+2}) ds_{k+2} \\
&= \prod_{j=k}^k \mathbf{1}_{s_j \notin \mathcal{T}_{j,w}} \nabla_w \mu_{k,w}(s_k) \nabla_{\xi_k} Q_k^{\pi_w, \psi_w}(s_k, \xi_k) \Big|_{\xi_k = \mu_{k,w}(s_k)} \\
&\quad + \int_{s_{k+1}} p(s_k \rightarrow s_{k+1} | \pi_w, \psi_w) \cdot \prod_{j=k}^{k+1} \mathbf{1}_{s_j \notin \mathcal{T}_{j,w}} \nabla_w \mu_{k+1,w}(s_{k+1}) \nabla_{\xi_{k+1}} Q_{k+1}^{\pi_w, \psi_w}(s_{k+1}, \xi_{k+1}) \Big|_{\xi_{k+1} = \mu_{k+1,w}(s_{k+1})} ds_{k+1} \\
&\quad + \int_{s_{k+2}} p(s_k \rightarrow s_{k+2} | \pi_w, \psi_w) \cdot \prod_{j=k}^{k+2} \mathbf{1}_{s_j \notin \mathcal{T}_{j,w}} \nabla_w \mu_{k+2,w}(s_{k+2}) \nabla_{\xi_{k+2}} Q_{k+2}^{\pi_w, \psi_w}(s_{k+2}, \xi_{k+2}) \Big|_{\xi_{k+2} = \mu_{k+2,w}(s_{k+2})} ds_{k+2} \\
&\quad \vdots \\
&\quad + \int_{s_N} p(s_k \rightarrow s_N | \pi_w, \psi_w) \prod_{j=k}^N \mathbf{1}_{s_j \notin \mathcal{T}_{j,w}} \nabla_w V_N^{\pi_w, \psi_w}(s_N) ds_N \\
&= \sum_{l=k}^{N-1} \int_{s_l} p(s_k \rightarrow s_l | \pi_w, \psi_w) \prod_{j=k}^l \mathbf{1}_{s_j \notin \mathcal{T}_{j,w}} \nabla_w \mu_{l,w}(s_l) \nabla_{\xi_l} Q_l^{\pi_w, \psi_w}(s_l, \xi_l) \Big|_{\xi_l = \mu_{l,w}(s_l)} ds_l \\
&= \sum_{l=k}^{N-1} \mathbb{E}_{s_l | \pi_w, \psi_w, s_k} \left[ \prod_{j=k}^l \mathbf{1}_{s_j \notin \mathcal{T}_{j,w}} \nabla_w \mu_{l,w}(s_l) \nabla_{\xi_l} Q_l^{\pi_w, \psi_w}(s_l, \xi_l) \Big|_{\xi_l = \mu_{l,w}(s_l)} \right]. \tag{56}
\end{aligned}$$

At last, we obtain the policy gradient expression:

$$\begin{aligned}
\nabla_w U(w) &= \nabla_w V_0^{\pi_w, \psi_w}(s_0) \\
&= \sum_{l=0}^{N-1} \mathbb{E}_{s_l | \pi_w, \psi_w, s_0} \left[ \prod_{j=0}^l (1 - \mathbf{1}_{s_j \in \mathcal{T}_{j,w}}) \nabla_w \mu_{l,w}(s_l) \nabla_{\xi_l} Q_l^{\pi_w, \psi_w}(s_l, \xi_l) \Big|_{\xi_l = \mu_{l,w}(s_l)} \right] \\
&= \sum_{l=0}^{N-1} \mathbb{E}_{s_l | \pi_w, \psi_w, s_0} \left[ \mathbf{1}_{l < \tau_w} \nabla_w \mu_{l,w}(s_l) \nabla_{\xi_l} Q_l^{\pi_w, \psi_w}(s_l, \xi_l) \Big|_{\xi_l = \mu_{l,w}(s_l)} \right].
\end{aligned} \tag{57}$$

□

#### A.4 Analytical solution to the linear-Gaussian problem

We derive the analytical solution to the linear-Gaussian problem described in Section 4.1, under the terminal reward formulation. The conjugate Gaussian structure enables us to obtain closed-form expressions for the optimal stopping and design policies. Due to this conjugacy, both the prior and posterior distributions remain Gaussian throughout the sequential process, with log-density functions given by:

$$\ln p(\theta | I_0) = -\frac{1}{2} \ln(2\pi\sigma_0^2) - \frac{(m_0 - \theta)^2}{2\sigma_0^2} \tag{58}$$

$$\ln p(\theta | I_k) = -\frac{1}{2} \ln(2\pi\sigma_k^2) - \frac{(m_k - \theta)^2}{2\sigma_k^2}, \tag{59}$$

where  $m_k$  and  $\sigma_k^2$  denote the posterior mean and variance after performing  $k$  experiments. These posterior parameters can be updated iteratively as:

$$(m_k, \sigma_k^2) = \left( \frac{\frac{y_{k-1}/\xi_{k-1} + m_{k-1}}{\sigma_\epsilon^2/\xi_{k-1}^2 + \frac{1}{\sigma_{k-1}^2}}, \frac{1}{\frac{1}{\sigma_\epsilon^2/\xi_{k-1}^2} + \frac{1}{\sigma_{k-1}^2}}} \right). \tag{60}$$

Alternatively, they can be computed directly from the complete experimental history:

$$\begin{aligned}
\sigma_k^2 &= \frac{\sigma_0^2 \sigma_\epsilon^2}{\sigma_\epsilon^2 + \sigma_0^2 \sum_{i=0}^{k-1} \xi_i^2} \\
m_k &= \sigma_k^2 \left( \frac{m_0}{\sigma_0^2} + \frac{1}{\sigma_\epsilon^2} \sum_{i=0}^{k-1} y_i \xi_i \right).
\end{aligned} \tag{61}$$

For Gaussian distributions, the KL divergence has a closed form expression:

$$D_{\text{KL}}(\mathcal{N}(m_a, \sigma_a^2) || \mathcal{N}(m_b, \sigma_b^2)) = \frac{1}{2} \left[ \frac{\sigma_a^2}{\sigma_b^2} + \frac{(m_a - m_b)^2}{\sigma_b^2} + \ln \frac{\sigma_b^2}{\sigma_a^2} - 1 \right]. \tag{62}$$

This closed form allows us to derive explicit expressions for the expected information gain. Since  $\sigma_{k+1}^2$  is updated independently of the observation  $y_k$  for all  $k$ , the expected information gain from performing experiment  $k$  is given by:

$$\begin{aligned}
&\mathbb{E}_{y_k | s_k, \xi_k} [D_{\text{KL}}(p_{\theta | I_{k+1}} || p_{\theta | I_k})] \\
&= \mathbb{E}_{y_k | s_k, \xi_k} \left[ \frac{1}{2} \left\{ \frac{\sigma_{k+1}^2}{\sigma_k^2} + \frac{(m_{k+1} - m_k)^2}{\sigma_k^2} + \ln \frac{\sigma_k^2}{\sigma_{k+1}^2} - 1 \right\} \right] \\
&= \frac{1}{2} \mathbb{E}_{y_k | s_k, \xi_k} \left[ \frac{(m_{k+1} - m_k)^2}{\sigma_k^2} \right] + \frac{1}{2} \left( \frac{\sigma_{k+1}^2}{\sigma_k^2} + \ln \frac{\sigma_k^2}{\sigma_{k+1}^2} - 1 \right) \\
&= \frac{1}{2} \mathbb{E}_{y_k | s_k, \xi_k} \left[ \frac{\sigma_k^2 (y_k / \xi_k - m_k)^2}{(\sigma_k^2 + \sigma_\epsilon^2 / \xi_k^2)^2} \right] + \frac{1}{2} \left( \frac{\sigma_{k+1}^2}{\sigma_k^2} + \ln \frac{\sigma_k^2}{\sigma_{k+1}^2} - 1 \right) \\
&= \frac{1}{2} \frac{\sigma_k^2 \xi_k^2}{\sigma_k^2 \xi_k^2 + \sigma_\epsilon^2} + \frac{1}{2} \left( \frac{\sigma_{k+1}^2}{\sigma_k^2} + \ln \frac{\sigma_k^2}{\sigma_{k+1}^2} - 1 \right) \\
&= \frac{1}{2} \left( 1 - \frac{\sigma_{k+1}^2}{\sigma_k^2} \right) + \frac{1}{2} \left( \frac{\sigma_{k+1}^2}{\sigma_k^2} + \ln \frac{\sigma_k^2}{\sigma_{k+1}^2} - 1 \right)
\end{aligned}$$

$$= \frac{1}{2} \ln \frac{\sigma_k^2}{\sigma_{k+1}^2} \quad (63)$$

in which computing the expectations utilizes the identities

$$\begin{aligned} \mathbb{E}_{y_k | m_k, \sigma_k^2, \xi_k} [y_k] &= \int_{-\infty}^{+\infty} y_k p(y_k | m_k, \sigma_k^2, \xi_k) dy_k \\ &= \int_{-\infty}^{+\infty} \int_{-\infty}^{+\infty} y_k p(y_k | \theta, m_k, \sigma_k^2, \xi_k) p(\theta | m_k, \sigma_k^2, \xi_k) dy_k d\theta \\ &= \int_{-\infty}^{+\infty} \xi_k \theta p(\theta | m_k, \sigma_k^2, \xi_k) d\theta \\ &= \xi_k m_k, \end{aligned} \quad (64)$$

and

$$\begin{aligned} \mathbb{E}_{y_k | m_k, \sigma_k^2, \xi_k} [y_k^2] &= \int_{-\infty}^{+\infty} y_k^2 p(y_k | m_k, \sigma_k^2, \xi_k) dy_k \\ &= \int_{-\infty}^{+\infty} \int_{-\infty}^{+\infty} y_k^2 p(y_k | \theta, m_k, \sigma_k^2, \xi_k) p(\theta | m_k, \sigma_k^2, \xi_k) dy_k d\theta \\ &= \int_{-\infty}^{+\infty} (\sigma_\epsilon^2 + \xi_k^2 \theta^2) p(\theta | m_k, \sigma_k^2, \xi_k) d\theta \\ &= \sigma_\epsilon^2 + \xi_k^2 (\sigma_k^2 + m_k^2). \end{aligned} \quad (65)$$

Using (63) we now present the first two steps in deriving the optimal sequential designs for the Linear-Gaussian case. For the last design,

$$\begin{aligned} \xi_{N-1}^* &= \arg \max_{\xi_{N-1}} Q_{N-1}^{\pi, \psi}(s_{N-1}, \xi_{N-1}) \\ &= \arg \max_{\xi_{N-1}} \mathbb{E}_{y_{N-1} | \xi_{N-1}} [V_N^{\pi, \psi}(s_N)] \\ &= \arg \max_{\xi_{N-1}} \left\{ \mathbb{E}_{y_{N-1} | \xi_{N-1}} [D_{\text{KL}}(p_{\theta | I_N} \| p_{\theta | I_0})] + \sum_{i=0}^{N-1} c_i(\xi_i) \right\} \\ &= \arg \max_{\xi_{N-1}} \left\{ D_{\text{KL}}(p_{\theta | I_{N-1}} \| p_{\theta | I_0}) + \sum_{i=0}^{N-2} c_i(\xi_i) + \mathbb{E}_{y_{N-1} | \xi_{N-1}} [D_{\text{KL}}(p_{\theta | I_N} \| p_{\theta | I_{N-1}})] + c_{N-1}(\xi_{N-1}) \right\} \\ &= \arg \max_{\xi_{N-1}} \left\{ \mathbb{E}_{y_{N-1} | \xi_{N-1}} [D_{\text{KL}}(p_{\theta | I_N} \| p_{\theta | I_{N-1}})] + c_{N-1}(\xi_{N-1}) \right\} \\ &= \arg \max_{\xi_{N-1}} \left\{ \frac{1}{2} \ln \frac{\sigma_{N-1}^2}{\sigma_N^2} + c_{N-1}(\xi_{N-1}) \right\} \\ &= \arg \max_{\xi_{N-1}} \left\{ \frac{1}{2} \ln \left[ \left( \frac{1}{\sigma_{N-1}^2} + \frac{\xi_{N-1}^2}{\sigma_\epsilon^2} \right) \sigma_{N-1}^2 \right] + c_{N-1}(\xi_{N-1}) \right\} \end{aligned} \quad (66)$$

which achieves optimality at the maximum value  $\xi_{N-1}^* = 3$  due to the monotone increasing property and design-independent costs. The corresponding maximum Q value is

$$Q_{N-1}^{\pi^*, \psi^*}(s_{N-1}, \xi_{N-1}^*) = D_{\text{KL}}(p_{\theta | I_{N-1}} \| p_{\theta | I_0}) + \frac{1}{2} \ln \frac{\sigma_{N-1}^2}{\sigma_N^{*2}} + c_{N-1}(\xi_{N-1}^*). \quad (67)$$

The stopping set for this stage is then

$$\begin{aligned} \mathcal{T}_{N-1}^{\pi^*, \psi^*} &= \left\{ s_{N-1} \mid r_T^S(s_{N-1}) \geq Q_{N-1}^{\pi^*, \psi^*}(s_{N-1}, \xi_{N-1}^*) \right\} \\ &= \left\{ s_{N-1} \mid 0 \geq \frac{1}{2} \ln \frac{\sigma_{N-1}^2}{\sigma_N^{*2}} + c_{N-1}(\xi_{N-1}^*) \right\}, \end{aligned} \quad (68)$$

which is independent of observations. Thus for stage  $N - 2$ ,

$$\begin{aligned} Q_{N-2}^{\pi, \psi}(s_{N-2}, \xi_{N-2}) &= \mathbb{E}_{y_{N-2} | \xi_{N-2}} \max \left\{ r_T^S(s_{N-1}), Q_{N-1}^{\pi^*, \psi^*}(s_{N-1}, \xi_{N-1}^*) \right\} \\ &= \max \left\{ \mathbb{E}_{y_{N-2} | \xi_{N-2}} [r_T^S(s_{N-1})], \mathbb{E}_{y_{N-2} | \xi_{N-2}} [Q_{N-1}^{\pi^*, \psi^*}(s_{N-1}, \xi_{N-1}^*)] \right\}. \end{aligned} \quad (69)$$

For the first case,

$$\begin{aligned} \xi_{N-2}^* &= \arg \max_{\xi_{N-2}} Q_{N-2}^{\pi, \psi}(s_{N-2}, \xi_{N-2}) \\ &= \arg \max_{\xi_{N-2}} \left\{ \mathbb{E}_{y_{N-2} | \xi_{N-2}} [D_{\text{KL}}(p_{\theta | I_{N-1}} \| p_{\theta | I_0})] + \sum_{i=0}^{N-2} c_i(\xi_i) \right\} \\ &= \arg \max_{\xi_{N-2}} \left\{ \mathbb{E}_{y_{N-2} | \xi_{N-2}} [D_{\text{KL}}(p_{\theta | I_{N-1}} \| p_{\theta | I_{N-2}})] + c_{N-2}(\xi_{N-2}) \right\} \\ &= \arg \max_{\xi_{N-2}} \left\{ \frac{1}{2} \ln \left[ \left( \frac{1}{\sigma_{N-2}^2} + \frac{\xi_{N-2}^2}{\sigma_\epsilon^2} \right) \sigma_{N-2}^2 \right] + c_{N-2}(\xi_{N-2}) \right\}; \end{aligned} \quad (70)$$

for the second case,

$$\begin{aligned} \xi_{N-2}^* &= \arg \max_{\xi_{N-2}} Q_{N-2}^{\pi, \psi}(s_{N-2}, \xi_{N-2}) \\ &= \arg \max_{\xi_{N-2}} \left\{ \mathbb{E}_{y_{N-2} | \xi_{N-2}} [D_{\text{KL}}(p_{\theta | I_{N-1}} \| p_{\theta | I_0})] + \frac{1}{2} \ln \left( \frac{\sigma_{N-1}^2}{\sigma_N^{*2}} \right) + c_{N-1}(\xi_{N-1}^*) \right\} \\ &= \arg \max_{\xi_{N-2}} \left\{ \frac{1}{2} \ln \frac{\sigma_{N-2}^2}{\sigma_{N-1}^2} + \frac{1}{2} \ln \left( \frac{\sigma_{N-1}^2}{\sigma_N^{*2}} \right) + c_{N-2}(\xi_{N-2}) + c_{N-1}(\xi_{N-1}^*) \right\} \\ &= \arg \max_{\xi_{N-2}} \left\{ \frac{1}{2} \ln \left[ \left( \frac{1}{\sigma_{N-2}^2} + \frac{\xi_{N-2}^2}{\sigma_\epsilon^2} + \frac{\xi_{N-1}^{*2}}{\sigma_\epsilon^2} \right) \sigma_{N-2}^2 \right] + c_{N-2}(\xi_{N-2}) \right\}. \end{aligned} \quad (71)$$

Both cases are equivalent in achieving the optimality at the maximum value  $\xi_{N-2}^* = 3$ , due to the monotone increasing property and design-independent costs. Iteratively we have

$$\xi_k^* = \arg \max_{\xi_k} \frac{1}{2} \ln \left[ \left( \frac{1}{\sigma_k^2} + \frac{\xi_k^2}{\sigma_\epsilon^2} \right) \sigma_k^2 \right] = 3, \quad \text{for } k = 0, \dots, N-1. \quad (72)$$

The stopping sets for each stage are

$$\begin{aligned} \mathcal{T}_k^{\pi^*, \psi^*} &= \left\{ s_k \mid 0 \geq \frac{1}{2} \ln \frac{\sigma_k^{*2}}{\sigma_{k+1}^{*2}} + c_k(\xi_k^*) \right\} \\ &= \left\{ s_k \mid 0 \geq \frac{1}{2} \ln \left( 1 + \frac{\sigma_k^{*2} \sigma_0^2}{\sigma_\epsilon^2 + \sigma_0^2 \sum_{i=0}^{k-1} \xi_i^{*2}} \right) + c_k(\xi_k^*) \right\} \end{aligned} \quad (73)$$

Finally the optimal utility for performing  $N$  experiments is

$$\begin{aligned} Q_0^*(s_0) &= \frac{1}{2} \ln \left[ \left( \frac{1}{\sigma_0^2} + \frac{\xi_0^2}{\sigma_\epsilon^2} + \frac{\xi_1^{*2}}{\sigma_\epsilon^2} + \dots + \frac{\xi_{N-1}^{*2}}{\sigma_\epsilon^2} \right) \sigma_0^2 \right] + \sum_{i=0}^{N-1} c_i(\xi_i^*) \\ &= \frac{1}{2} \ln \left( \sigma_\epsilon^2 + \sigma_0^2 \sum_{i=0}^{N-1} \xi_i^{*2} \right) - \frac{1}{2} \ln \sigma_\epsilon^2 + \sum_{i=0}^{N-1} c_i(\xi_i^*). \end{aligned} \quad (74)$$

## A.5 Hyperparameters

The hyperparameters used for training are given in Table 2.

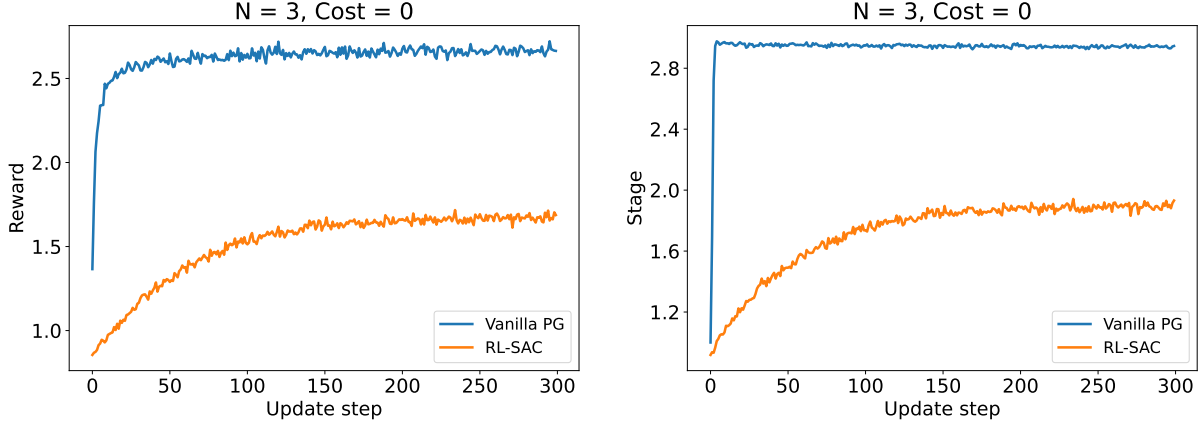


Figure 15: Performance comparison between Vanilla PG (our method) and a generic RL baseline (soft actor-critic) on the linear-Gaussian benchmark with zero experimental cost ( $c_k = 0$ ). Left: average reward; right: average stopping stage.

Table 2: Hyperparameter settings for numerical experiments.

	Linear Gaussian	Nonlinear	Source Detection
Policy network architecture	$N + (N - 1)(N_x + N_y) \rightarrow 80 \rightarrow 80 \rightarrow N_x$		
Q-network architecture	$N + (N - 1)(N_x + N_y) + N_x \rightarrow 80 \rightarrow 80 \rightarrow 1$		
Learning rate (policy)	$1.5 \times 10^{-1}$		
Learning rate (critic)	$1.0 \times 10^{-3}$		
Critic batch size	500		
Exploration scale $\sigma_{\text{explore}}$	1.0		0.05
Exploration scale decay	0.99		
Monte Carlo size $M$	1000		

## A.6 Additional results

While direct baselines for learned stopping in sequential experimental design are scarce in the literature, we construct a principled comparator by formulating stopping as part of the action space within a generic reinforcement learning framework. Specifically, we augment the action with a discrete stop or continue decision modeled by a stochastic policy, coupled with a continuous design policy for experiment selection. Both components are trained under a Soft Actor-Critic (SAC) (Haarnoja, Zhou, Abbeel and Levine, 2018) objective, yielding a unified hybrid-control baseline that does not rely on problem-specific stopping heuristics. Figure 15 presents the comparison on the linear-Gaussian benchmark. Even in this relatively simple setting, the SAC baseline performs substantially worse than our vanilla policy gradient. It fails to identify the optimal stopping stage and consequently achieves a lower total reward.

This behavior reflects a concrete difficulty that arises when applying a standard MDP formulation to stopping problems in sequential BED. The hybrid action space, which combines continuous experimental designs with a discrete stop or continue decision, forces generic policy gradient methods to represent stopping through a stochastic policy, since discrete actions cannot be differentiated directly. This is inconsistent with Theorem 3.1, which establishes that the optimal stopping policy is deterministic. Our key theoretical contribution is to exploit this structure to bypass the hybrid optimization problem altogether. By showing that the stopping policy is implicitly determined by the design policy, we reduce the joint optimization to a single gradient based update over the continuous design parameters alone, for which efficient pathwise estimators apply. The SAC baseline confirms that this reduction is not merely a modeling convenience. Without exploiting this structure, the mismatch between stochastic stopping and deterministic optimality leads to substantially suboptimal performance even on the simple linear Gaussian benchmark.

## References

Alexanderian, A., 2021. Optimal experimental design for infinite-dimensional Bayesian inverse problems governed by PDEs: A review. *Inverse Problems* 37, 043001.

- Audibert, J.Y., Bubeck, S., 2010. Best arm identification in multi-armed bandits, in: COLT-23th Conference on Learning Theory, pp. 41–53.
- Baldassari, L., Siahkoohi, A., Garnier, J., Solna, K., de Hoop, M.V., 2023. Conditional score-based diffusion models for bayesian inference in infinite dimensions. *Advances in Neural Information Processing Systems* 36, 24262–24290.
- Bengio, Y., Louradour, J., Collobert, R., Weston, J., 2009. Curriculum learning, in: *Proceedings of the 26th Annual International Conference on Machine Learning*, Association for Computing Machinery, New York, NY, USA. pp. 41–48.
- Berry, D.A., Müller, P., Grieve, A.P., Smith, M., Parke, T., Blazek, R., Mitchard, N., Krams, M., 2002. *Adaptive Bayesian Designs for Dose-Ranging Drug Trials*. Springer New York. pp. 99–181.
- Bertsekas, D., 2012. *Dynamic Programming and Optimal Control: Volume I*. Athena scientific.
- Blau, T., Bonilla, E.V., Chades, I., Dezfouli, A., 2022. Optimizing sequential experimental design with deep reinforcement learning, in: *Proceedings of the 39th International Conference on Machine Learning (ICML 2022)*, pp. 2107–2128.
- Chaloner, K., Verdinelli, I., 1995. Bayesian experimental design: A review. *Statistical Science* 10, 273–304.
- Daskalakis, C., Kawase, Y., 2017. Optimal stopping rules for sequential hypothesis testing, in: *25th Annual European Symposium on Algorithms (ESA)*.
- Evans, L.C., 2022. *Partial differential equations*. volume 19. American mathematical society.
- Fathan, A., Delage, E., 2021. Deep reinforcement learning for optimal stopping with application in financial engineering. arXiv preprint arXiv:2105.08877 .
- Foster, A., Ivanova, D.R., Malik, I., Rainforth, T., 2021. Deep adaptive design: Amortizing sequential Bayesian experimental design, in: *Proceedings of the 38th International Conference on Machine Learning (ICML 2021)*, pp. 3384–3395.
- Foster, A., Jankowiak, M., Bingham, E., Horsfall, P., Teh, Y.W., Rainforth, T., Goodman, N., 2019. Variational bayesian optimal experimental design. *Advances in neural information processing systems* 32.
- Frazier, P.I., Powell, W.B., Dayanik, S., 2008. A knowledge-gradient policy for sequential information collection. *SIAM Journal on Control and Optimization* 47, 2410–2439.
- Garnett, R., 2023. *Bayesian optimization*. Cambridge University Press.
- Haarnoja, T., Zhou, A., Abbeel, P., Levine, S., 2018. Soft actor-critic: Off-policy maximum entropy deep reinforcement learning with a stochastic actor, in: Dy, J., Krause, A. (Eds.), *Proceedings of the 35th International Conference on Machine Learning*, PMLR. pp. 1861–1870.
- Haggstrom, G.W., 1966. Optimal stopping and experimental design. *The Annals of Mathematical Statistics* , 7–29.
- Huan, X., Jagalur, J., Marzouk, Y., 2024. Optimal experimental design: Formulations and computations. *Acta Numerica* 33, 715–840.
- Ivanova, D.R., Foster, A., Kleinegesse, S., Gutmann, M.U., Rainforth, T., 2021. Implicit deep adaptive design: Policy-based experimental design without likelihoods, in: *Advances in Neural Information Processing Systems* 34, pp. 25785–25798.
- Kleinegesse, S., Gutmann, M.U., 2021. Gradient-based bayesian experimental design for implicit models using mutual information lower bounds. arXiv preprint arXiv:2105.04379 .
- Krause, A., Singh, A., Guestrin, C., 2008. Near-optimal sensor placements in gaussian processes: Theory, efficient algorithms and empirical studies. *Journal of Machine Learning Research* 9.
- Li, X., Lee, C.G., 2023.  $\delta v$ -learning: an adaptive reinforcement learning algorithm for the optimal stopping problem. *Expert Systems with Applications* 231, 120702.
- Lindley, D.V., 1956. On a Measure of the Information Provided by an Experiment. *The Annals of Mathematical Statistics* 27, 986–1005.
- Lookman, T., Balachandran, P.V., Xue, D., Yuan, R., 2019. Active learning in materials science with emphasis on adaptive sampling using uncertainties for targeted design. *npj Computational Materials* 5, 21.
- Murphy, S.A., 2003. Optimal dynamic treatment regimes. *Journal of the Royal Statistical Society Series B: Statistical Methodology* 65, 331–355.
- Peskir, G., Shiryaev, A., 2006. *Optimal Stopping and Free-boundary Problems*. Springer.
- Pullar-Strecker, Z., Dost, K., Frank, E., Wicker, J., 2024. Hitting the target: Stopping active learning at the cost-based optimum. *Machine Learning* 113, 1529–1547.

- Puterman, M.L., 2014. Markov Decision Processes: Discrete Stochastic Dynamic Programming. John Wiley & Sons.
- Rainforth, T., Foster, A., Ivanova, D.R., Smith, F.B., 2024. Modern Bayesian experimental design. *Statistical Science* 39, 100–114.
- Reed, M., Simon, B., Simon, B., Simon, B., 1972. *Methods of modern mathematical physics. volume 1.* Elsevier.
- Ryan, E.G., Drovandi, C.C., McGree, J.M., Pettitt, A.N., 2016. A review of modern computational algorithms for Bayesian optimal design. *International Statistical Review* 84, 128–154.
- Ryzhov, I.O., Powell, W.B., Frazier, P.I., 2012. The knowledge gradient algorithm for a general class of online learning problems. *Operations Research* 60, 180–195.
- Shen, W., Dong, J., Huan, X., 2025. Variational sequential optimal experimental design using reinforcement learning. *Computer Methods in Applied Mechanics and Engineering* 444, 118068.
- Shen, W., Huan, X., 2023. Bayesian sequential optimal experimental design for nonlinear models using policy gradient reinforcement learning. *Computer Methods in Applied Mechanics and Engineering* 416, 116304.
- Shiryayev, A.N., 2008. *Optimal Stopping Rules.* Springer.
- Silver, D., Lever, G., Heess, N., Degris, T., Wierstra, D., Riedmiller, M., 2014. Deterministic policy gradient algorithms, in: *Proceedings of the 31st International Conference on Machine Learning*, pp. 387–395.
- Sutton, R.S., Barto, A.G., 2018. *Reinforcement Learning: An Introduction.* MIT press.
- Wang, L., Cai, Q., Yang, Z., Wang, Z., 2020. Neural policy gradient methods: Global optimality and rates of convergence, in: *International Conference on Learning Representations.*
- Xie, Q., Cai, L., Terenin, A., Frazier, P.I., Scully, Z., 2025. Cost-aware stopping for bayesian optimization. arXiv preprint arXiv:2507.12453 .
- Zhu, J., Wang, H., Hovy, E., Ma, M., 2010. Confidence-based stopping criteria for active learning for data annotation. *ACM Transactions on Speech and Language Processing (TSLP)* 6, 1–24.